Further Studies on Imidazo[4,5-*b*]pyridine AT_1 Angiotensin II Receptor Antagonists. Effects of the Transformation of the 4-Phenylquinoline Backbone into 4-Phenylisoquinolinone or 1-Phenylindene Scaffolds

Andrea Cappelli,*[,†] Gal.la Pericot Mohr,[†,#] Germano Giuliani,[†] Simone Galeazzi,[†] Maurizio Anzini,[†] Laura Mennuni,[‡] Flora Ferrari,[‡] Francesco Makovec,[‡] Eva M. Kleinrath,[§] Thierry Langer,[§] Massimo Valoti,[||] Gianluca Giorgi,[⊥] and Salvatore Vomero[†]

Dipartimento Farmaco Chimico Tecnologico and European Research Centre for Drug Discovery and Development, Università di Siena, Via A. Moro, 53100 Siena, Italy, Rotta Research Laboratorium S.p.A., Via Valosa di Sopra 7, 20052 Monza, Italy, Department of Pharmaceutical Chemistry, Institute of Pharmacy, University of Innsbruck, Innrain 52a, A-6020 Innsbruck, Austria, Dipartimento di Scienze Biomediche, Università di Siena, Via A. Moro, 53100 Siena, Italy, and Dipartimento di Chimica, Università di Siena, Via A. Moro, 53100 Siena, Italy

Received March 20, 2006

The 4-phenylquinoline fragment of novel AT_1 receptor antagonists **4** based on imidazo[4,5-*b*]pyridine moiety was replaced by 4-phenylisoquinolinone (compounds **5**) or 1-phenylindene (compounds **6**) scaffolds to investigate the structure−activity relationships. Binding studies showed that most of the synthesized compounds display high affinity for the AT_1 receptor. Because of the in vitro high potency of carboxylic acids **5b**,**f**, they were evaluated in permeability (in Caco-2 cells) and in pharmacokinetic studies in comparison with quinoline derivatives **4b**,**i**,**j**,**k**. The studies showed that these compounds are characterized by rapid excretion, low membrane permeability, and low oral bioavailability. The structure optimization of the indene derivatives led to compounds **6e**,**f** possessing interesting AT_1 receptor affinities. Optimization produced polymerizing AT_1 receptor ligand **6c**, which forms a thermoreversible polymer (poly-**6c**) and is released from the latter by a temperature-dependent kinetics. The results suggest the possibility of developing novel polymeric prodrugs based on a new release mechanism. Finally, a set of 34 AT_1 receptor antagonists was used as a new test for the evaluation of the predictive capability of the previously published qualitative and quantitative pharmacophore models.

Introduction

Angiotensin II (Ang II) is an octapeptide produced by the renin-angiotensin system (RAS), which plays a key role in the pathophysiology of hypertension. In humans, Ang II interacts with two main receptor subtypes: AT_1 and AT_2.[1] The AT_1 receptor subtype mediates virtually all the known physiological actions of Ang II in cardiovascular, neuronal, endocrine, and hepatic cells as well as in other ones. This receptor belongs to the G-protein-coupled receptor (GPCR) superfamily and shows the seven hydrophobic transmembrane domains forming α-helices in the lipid bilayer of the cell membrane. The interaction of Ang II with the AT_1 receptor induces a conformational change, which promotes the coupling with the G protein(s) and leads to the signal transduction via several effector systems (phospholipases C, D, A2, adenyl cyclase etc.).[1,2]

The parallel discovery of losartan and eprosartan, potent and orally active nonpeptide Ang II antagonists, has stimulated the design of a large number of congeners.[3] Among them, irbesartan, candesartan, valsartan, telmisartan, and olmesartan are on the market and some 20 other compounds are being developed. The biphenyl fragment bearing an acidic moiety (tetrazole ring, −COOH, $-SO_2$-NH-CO−) is common to most of these compounds, which differ in the nature of the pendent heterocyclic system (valsartan lacks the heterocyclic moiety) connected to the para position of the distal phenyl by means of a methylene group. In fact, in the design of new nonpeptide Ang II antagonists, the strategy followed by most medicinal chemists was concerned with the molecular modification of the imidazole moiety of losartan (**1**). Among the large variety of the heterocyclic systems developed, an outstanding position is occupied by the imidazo[4,5-*b*]pyridine moiety of compound **2a** (L-158,809).[4] This congener of losartan has been reported to show a subnanomolar AT_1 receptor affinity about 1 order of magnitude higher than that of losartan and represents one of the most potent nonpeptide Ang II antagonists so far developed. This suggests that the stereoelectronic characteristics of the imidazo[4,5-*b*]pyridine moiety can be considered optimal for the interaction with the receptor. However, relatively little information is available on the effects of the molecular modification of the phenyl group bearing the acidic moiety (distal phenyl ring). Moreover, 4-phenyl-3-tetrazolylpyridyl derivative **2d** was reported to be a very potent Ang II antagonist showing, however, a somewhat poorer oral bioavailability than **2c** (L-158,338). The authors suggested elsewhere that the decrease in lipophilicity has a negative effect on the oral potency of compound **2d** with respect to **2c**.[5]

These observations led to some molecular modifications involving the distal phenyl group of compounds **2** and ultimately to the development of compounds **4**.[6] Some members of this series of 4-phenylquinoline derivatives showed in vitro properties comparable to those shown by losartan. However, pharmacokinetic studies performed with the selected candidate for further preclinical studies (CR3210, **4b**) showed a relatively low oral bioavailability and a rapid excretion.[7,8] Owing to the very interesting in vitro properties of quinoline derivatives **4**, the program of structural modification was pursued with the synthesis of both isoquinolinone derivatives **5** and indene

* To whom correspondence should be addressed. Tel: +39 0577 234320. Fax: +39 0577 234333. E-mail: cappelli@unisi.it.

† Dipartimento Farmaco Chimico Tecnologico and European Research Centre for Drug Discovery and Development, Università di Siena.

‡ Rotta Research Laboratorium S.p.A..

§ University of Innsbruck.

|| Dipartimento di Scienze Biomediche, Università di Siena.

⊥ Dipartimento di Chimica, Università di Siena.

Present address: Medicinal Chemistry, Siena Biotech, Via Torre Fiorentina 1, 53100 Siena, Italy.

10.1021/jm0603163 CCC: $33.50
Published on Web 10/06/2006

Chart 1. Structure of the AT_1 Receptor Antagonists Losartan, Valsartan, and Compounds **2**,**4**

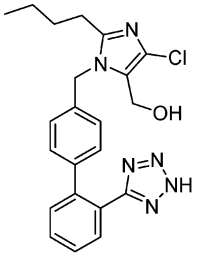

losartan (**1**)

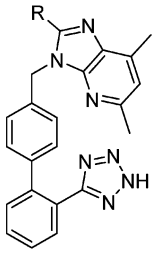

2a (L-158,809: R = C_2H_5)
2b (R = *n*-C_3H_7)

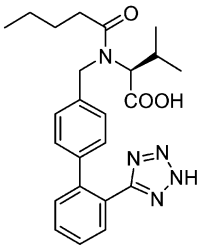

valsartan (**3**)

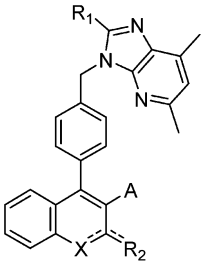

4

Chart 2. Structure and AT_1 Receptor Affinity of Compounds **2c**, **2d**, and **4b**

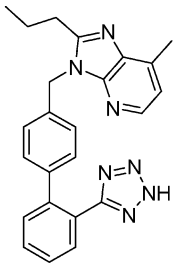

2c (L-158,338)
IC_{50} = 1 nM

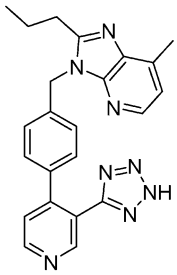

2d
4 nM

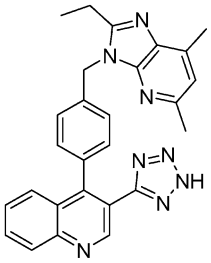

4b (CR3210)
6.9 nM

Chart 3. Structure of the Newly Synthesized Isoquinolinone Derivatives **5** and Indene Derivatives **6**

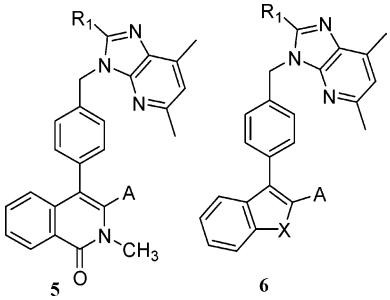

5 **6**

derivatives **6** as a further step of an investigation devoted to both the development of new antihypertensive agents and the understanding of the molecular basis of their pharmacodynamic and pharmacokinetic[9] properties.In this article, the synthesis, the preliminary pharmacological characterization, and the deduction of structure−affinity relationships (SAFIR) of the novel Ang II antagonists **5** and **6** are described together with an assessment study of the prediction capability of our previously published qualitative and quantitative pharmacophore models.[10]

Scheme 1[a]

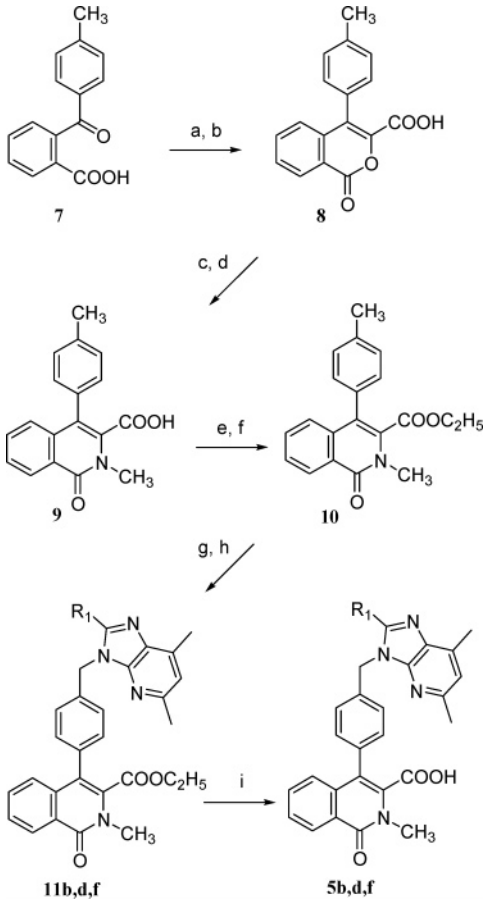

[a] Reagents: (a) Br-CH($COOC_2H_5$)$_2$, K_2CO_3, CH_3COCH_3; (b) HCl, CH_3COOH; (c) CH_3NH_2, C_2H_5OH; (d) H_2SO_4, C_2H_5OH; (e) $SOCl_2$, CH_2Cl_2; (f) C_2H_5OH, $(C_2H_5)_3N$; (g) NBS, dibenzoyl peroxide, CCl_4; (h) 2-substituted-5,7-dimethyl-3*H*-imidazo[4,5-*b*]pyridine, NaH, DMF; (i) NaOH, C_2H_5OH.

Results

Chemistry. The preparation of isoquinoline-3-carboxylic acid derivatives **5b**,**d**,**f** was carried out starting from the commercially available 2-(*p*-toluoyl)benzoic acid **7** as described in Scheme 1.

Acid **7** was transformed into isocoumarin-3-carboxylic acid (**8**), which was reacted with methylamine and dehydrated to acid **9** by modifying a procedure described in the literature.[11] The corresponding ester **10** was easily obtained from **9** and subjected to the standard bromination-coupling-deprotection procedure (BCD: benzylic bromination, coupling reaction with substituted imidazo[4,5-*b*]pyridine derivatives,[4,6,12] and unmasking of the acidic moiety) to obtain the target isoquinoline-3-carboxylic acid derivatives **5b**,**d**,**f**.

However, 3-tetrazolylisoquinoline derivatives **5a**,**c**,**e** were obtained by means of a multistep procedure[11] involving the formation of 3-cyanoisoquinolone derivative **12** (Scheme 2). The application of the classical tetrazole chemistry to **12** led to protected tetrazole intermediate **13**, which was subjected to the standard BCD procedure to give target derivatives **5a**,**c**,**e**.

Indenone derivatives **6a**,**b** were synthesized by applying the BCD procedure to *tert*-butyl ester **14**, which was prepared by modifying the procedure described for the preparation of the corresponding ethyl ester (ethyl 3-(4-methylphenyl)-1-oxo-1*H*-indene-2-carboxylate).[13]

Schemes 4−7 describe the elaboration of the intermediate indenone derivative **15b** designed to explore the top of the AT_1 receptor binding cavity further, where the basic amino acid

Scheme 2[a]

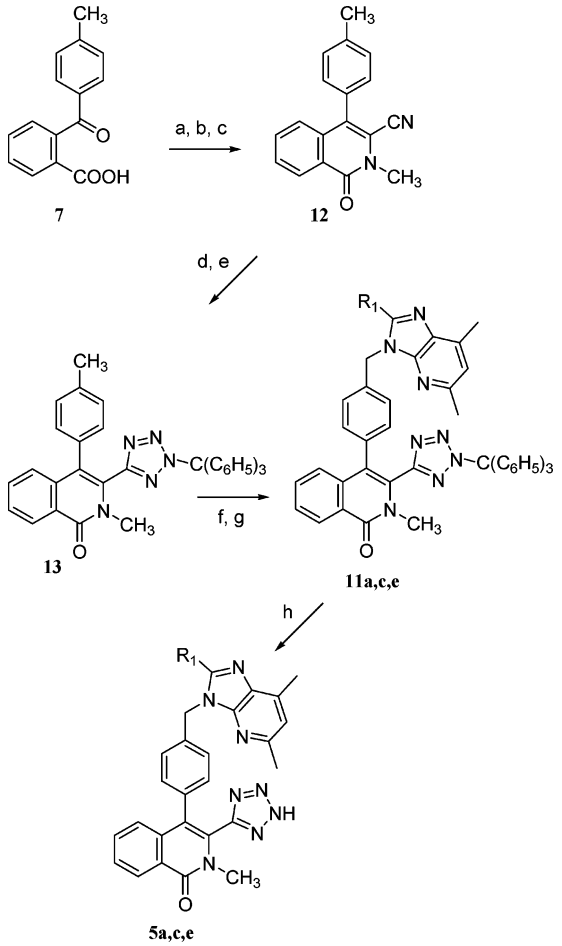

[a] Reagents: (a) $SOCl_2$, CH_2Cl_2; (b) $CH_3NHCH_2CN{\cdot}HCl$, TEA, CH_2Cl_2; (c) DBU, toluene; (d) $(CH_3)_3SnN_3$, xylene; (e) $(C_6H_5)_3CCl$, NaOH, THF, CH_2Cl_2; (f) NBS, dibenzoyl peroxide, CCl_4; (g) 2-substituted-5,7-dimethyl-3*H*-imidazo[4,5-*b*]pyridine, NaH, DMF; (h) HCOOH.

Lys199 establishes the ion−pair interaction with the acidic moiety of the antagonist.[6] On the basis of the intriguing results obtained with related 2-indenecarboxylic acid derivatives (e.g., **BF1**, Scheme 4),[13,14] this synthetic work, at the same time, can be considered an exploration of the chemical behavior of these indene derivatives. In particular, we were interested in evaluating (a) the stability of *trans*-diene **6c**, (b) its propensity to spontaneous polymerization, and (c) the characteristics of the thermo-induced depolymerization process. In fact, we previously found that **BF1** was stable in solution, but polymerized spontaneously upon solvent removal to give poly-**BF1**, a new polymer showing interesting properties such as thermoreversible polymerization/depolymerization behavior, high solubility in the most common organic solvents, a π-stacked structure, and liability to give nanostructured aggregates.[13,14] Moreover, **BF1** showed the tendency to behave as a Michael acceptor and, in the presence of a nucleophile such as *N*-methylpiperazine, established an equilibrium with its adducts.[14] This chemical behavior of **BF1**, taken together with the presence of the basic Lys199 on the top of the AT_1 receptor binding cavity, shows the importance of the chemical studies and the biological characterization of **6c**.

Trans-diene **6c** was obtained in trace amounts from the deprotection reaction with formic acid of ester **16e** to acid **6e** and in more substantial amounts by dehydration of **16e** or acid **6e** in the presence of *p*-toluenesulfonic acid (PTSA) in $CHCl_3$

Scheme 3[a]

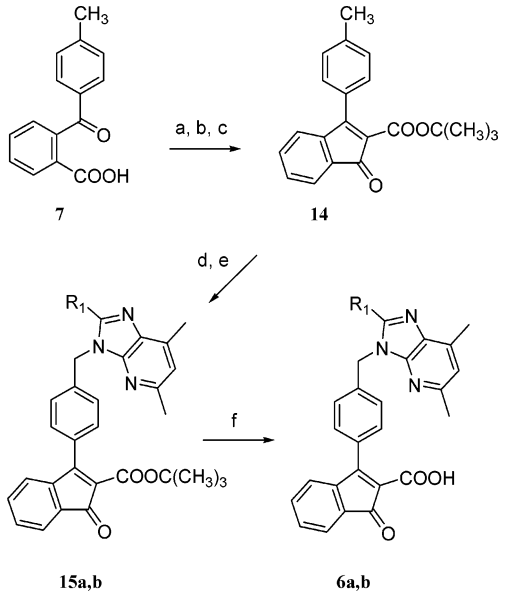

[a] Reagents: (a) $SOCl_2$, CH_2Cl_2; (b) $C_2H_5OMgCH(COOt\text{-}Bu)_2$, $C_2H_5OC_2H_5$; (c) K_2CO_3, C_2H_5OH; (d) NBS, dibenzoyl peroxide, CCl_4; (e) 2-substituted-5,7-dimethyl-3*H*-imidazo[4,5-*b*]pyridine, NaH, DMF; (f) HCOOH.

Scheme 4[a]

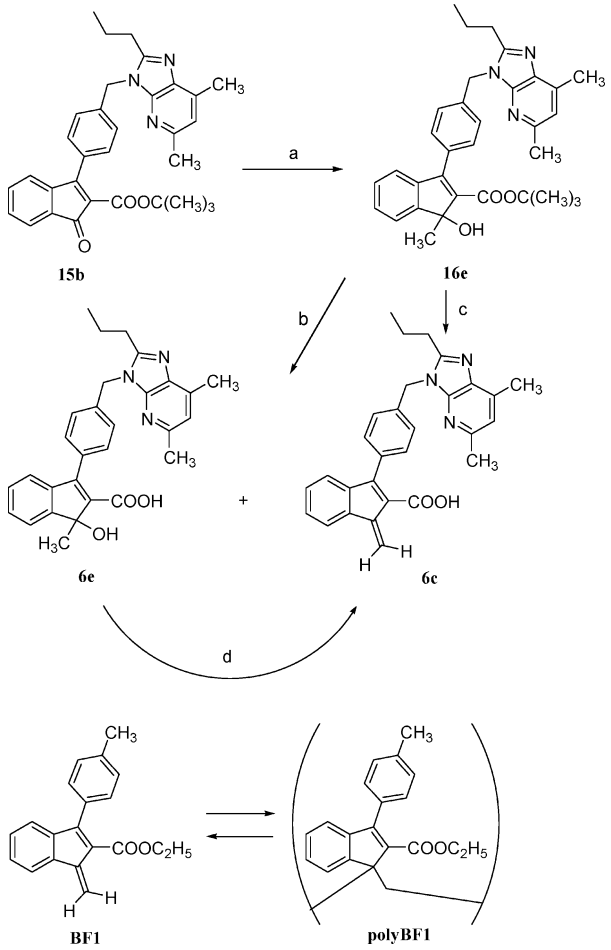

[a] Reagents: (a) $Al(CH_3)_3$, CH_2Cl_2; (b) HCOOH; (c) PTSA, $CHCl_3$; (d) PTSA, $CDCl_3$.

(or $CDCl_3$). Interestingly, benzofulvene derivative **6c** was stable as a pure crystalline solid but polymerized spontaneously when the mixture of the dehydration reaction of **6e** was concentrated without the elimination of PTSA. Because the ethyl ester of

acid **6c** showed the same spontaneous polymerization behavior as that of **BF1** (see Supporting Information), we assume that the stability of pure **6c** is related to the possible intermolecular interaction of its COOH with the imidazole nitrogen in the solid state otherwise prevented by the presence of PTSA, which protonates the heterocyclic nitrogens. This assumption is supported by the crystal structure of a previously published quinoline derivative in which the same intermolecular interaction stabilizes the crystal packing.[6] The polymer substance obtained (poly-**6c**·PTSA) was characterized by ^{1}H NMR spectroscopy (e.g., thermal-induced depolymerization followed by ^{1}H NMR at 200 MHz, Figure 1). When a solution of poly-**6c**−PTSA in DMSO-d_6 was heated at different temperatures, the depolymerization of poly-**6c** occurred at different velocities as demonstrated by the appearance of the signals typical of **6c** (Figure 1). At 55 °C, the depolymerization process was very slow, while becoming significantly more rapid at 80 °C; at 140 °C, it is even faster because it was almost complete after 1 h of heating. At 120 °C, the fragmentation process showed an intermediate velocity and it could be profitably followed by ^{1}H NMR spectroscopy, which clearly showed that the reaction reached equilibrium after 4 h of heating (Figure 1). For poly-**6c**, these results suggest a thermoreversible polymerization/depolymerization behavior similar to that shown by poly-**BF1** but characterized by a faster kinetics.

The hydrogenation of acid **6c** generated in situ from ester **16e** with PTSA in toluene gave a mixture of dihydro derivatives **6d** (the product of the hydrogenation in positions 1,2 of the diene fragment) and **17** (the compound hydrogenated in positions 1,4 of the diene fragment), which were separated by flash chromatography (Scheme 5).

Ester **15b** was reacted with the anion of the di-*tert*-butyl malonate to give **18**, which was cleaved with formic acid to diacid **20** (Scheme 7) or with hydrochloric acid in acetic acid to obtain monoacid **19**. The structure of the latter compound was confirmed by single-crystal X-ray diffraction studies. In fact, monoacid **19** crystallized from ethyl acetate to give single crystals suitable for X-ray diffraction studies (Figure 2), whereas diacid **20** did not. Therefore, the synthetic procedure used in the preparation of **20** was applied to the synthesis of the simplified analogue **21** lacking the imidazo[4,5-*b*]pyridine moiety, and X-ray quality crystals were obtained from chloroform (Figure 3).

Finally, acylsulfonamide derivatives **6g**,**h** were synthesized by reaction of carboxylic acid **6b** with the appropriate sulfonamide in the presence of EDCI and DMAP (Scheme 7).

Structure−Affinity Relationship Studies. The newly synthesized bicyclic derivatives **5a**−**f**, **6a**−**h**, **17**, **19**, and **20** (showing a suitable degree of purity as confirmed by ^{1}H NMR and combustion analyses) were tested for their potential ability to displace [^{125}I]Sar1,Ile8-Ang II specifically bound to the AT_1 receptor in rat hepatic membranes in comparison with reference compounds losartan, and valsartan, following well-established protocols.[15] The results of the binding studies are summarized in Table 1 along with the affinities of some of the previously published compounds **4a**−**n**, which are included for comparative purposes. The results show that most of the tested compounds displayed high affinity for the AT_1 receptor, although lower than that of reference compound **2a**.

(a) Effects of the Modification of the Quinoline Moiety of Compounds 4. In our previous article,[6] we reported that the introduction of an additional benzene ring into the structure of carboxylic acid derivative **2c** leading to naphthalene derivative **4a**[16] was tolerated by the receptor, and the transformation of the naphthalene moiety of **4a** into the quinoline one of **4c** had slightly positive effects. The results obtained with the newly synthesized compounds show that the isoquinolinone moiety of compounds **5b**,**d**,**f** is better accommodated by the receptor than benzene, naphthalene, and quinoline groups of compounds **2**,**4**, indicating this molecular portion as an optimized group for the interaction with the top of the AT_1 receptor binding cavity. The comparison between compounds **5b** and **4f** shows the importance of the correct position/orientation of the carbonyl dipole, which in compounds **5** occupies the position of quinoline

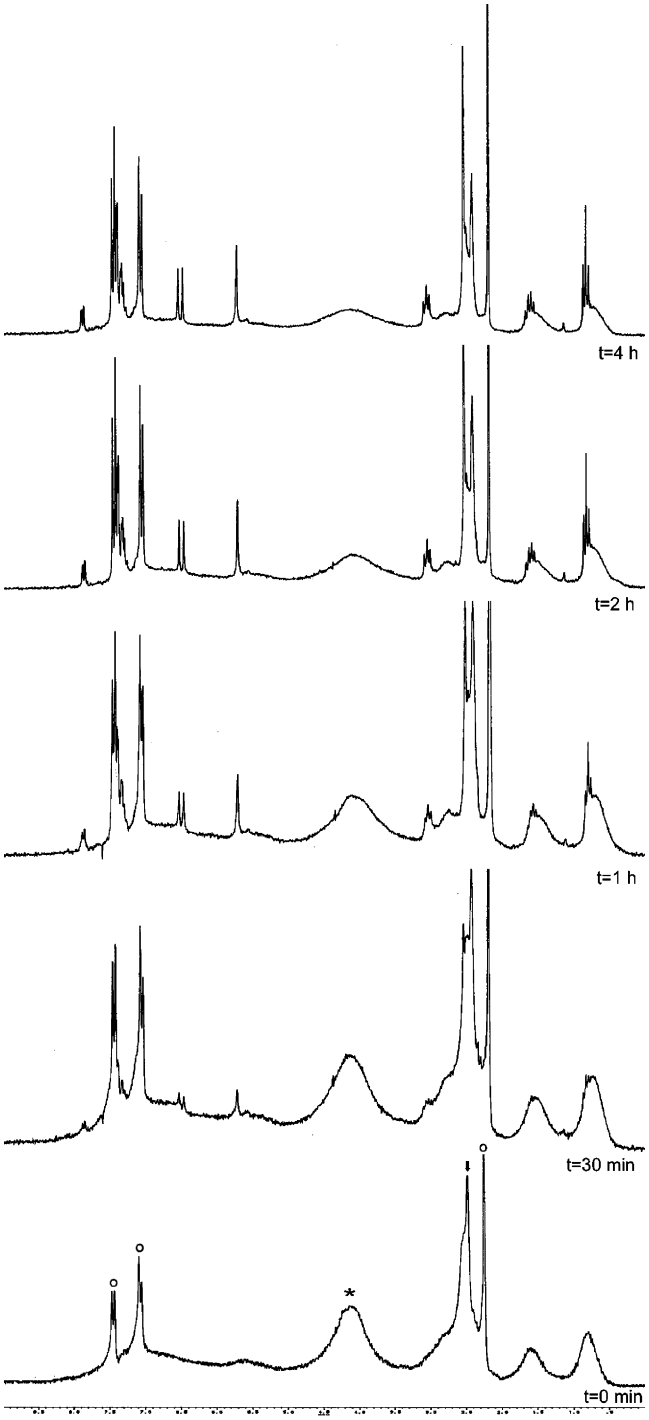

Figure 1. Thermo-induced depolymerization of poly-**6c**, followed by ^{1}H NMR (200 MHz). A solution of 2.5 mg of poly-**6c**−PTSA in 0.5 mL of (DMSO-d_6) was heated at 120 °C, and ^{1}H NMR spectra were recorded at regular time intervals. The arrow indicates the solvent peak, the asterisk the water peak, and the empty circles the signals attributable to PTSA.

Scheme 5[a]

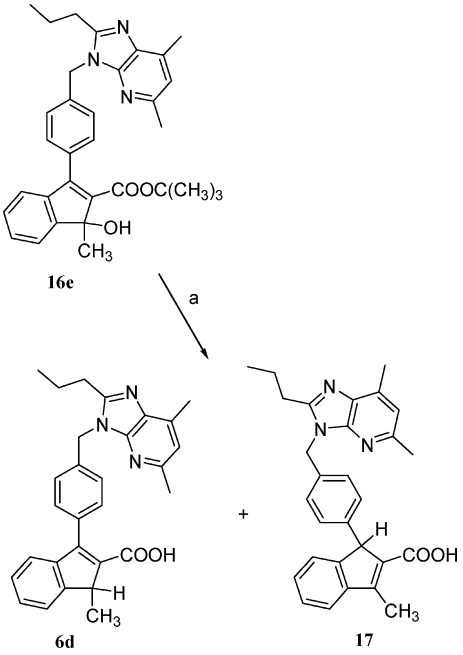

[a] Reagents: (a) H_2, Pd/C, PTSA, toluene.

Scheme 6[a]

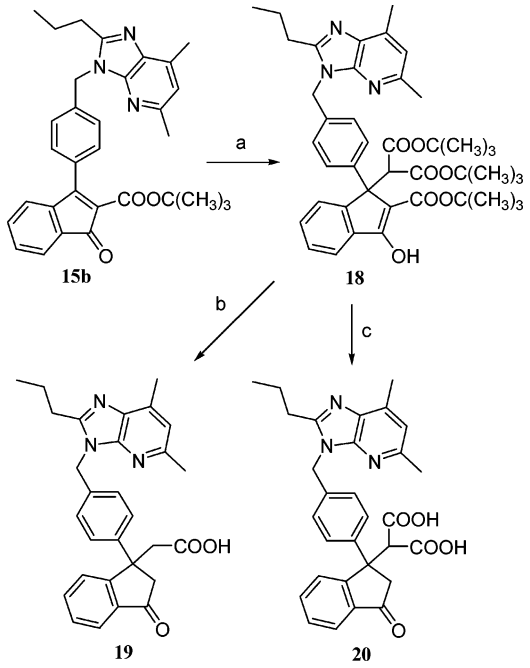

[a] Reagents: (a) $CH_2[COOC(CH_3)_3]_2$, NaH, THF; (b) HCl, CH_3COOH; (c) HCOOH.

nitrogen of compounds **4**. The deletion of the N-CH_3 group of compounds **5b**,**d** leading to **6a**,**b** produces a decrease in AT_1 receptor affinity of about 1 order of magnitude, whereas the transformation of the C═O group of the latter compounds into the tertiary carbinol group of **6e**,**f** restores high affinity. Comparison of the **6e** affinity (IC_{50} = 11 nM) with that shown by **6d** (IC_{50} = 99 nM), which lacks the hydroxyl group, shows the importance of this OH group in the interaction with the AT_1 receptor. The replacement of the carbonyl oxygen atom of **6b** with an exocyclic methylene group (e.g., compound **6c**) as well as the hybridization change of the carbon atom bearing the phenyl spacer (compare **6c** with **17**) has a negligible effect on AT_1 receptor affinity. Finally, the structure−affinity relationships

Scheme 7[a]

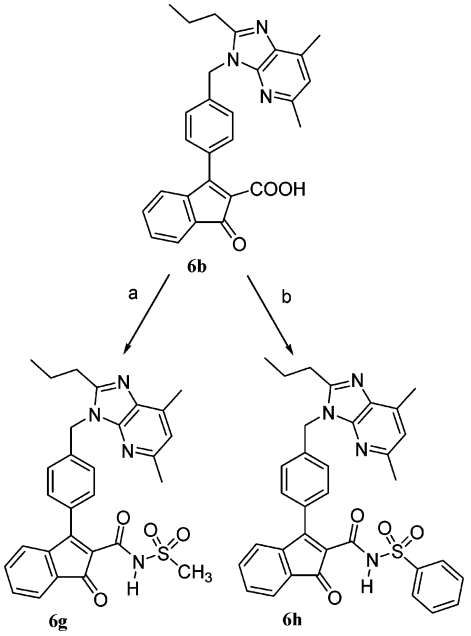

[a] Reagents: (a) CH_3-SO_2-NH_2, EDCI, DMAP, CH_2Cl_2; (b) C_6H_5-SO_2-NH_2, EDCI, DMAP, CH_2Cl_2.

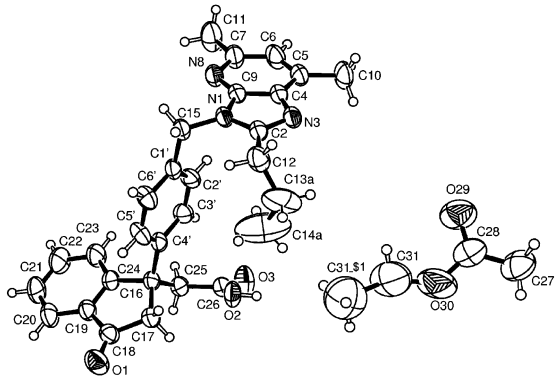

Figure 2. Crystal structure of **19**−0.5 $CH_3COOC_2H_5$. For the pendant ethyl moiety (−C(13)H_2-C(14)H_3), atoms having site occupation factor equal to 0.54(1) are reported. Ellipsoids enclose 50% probability.

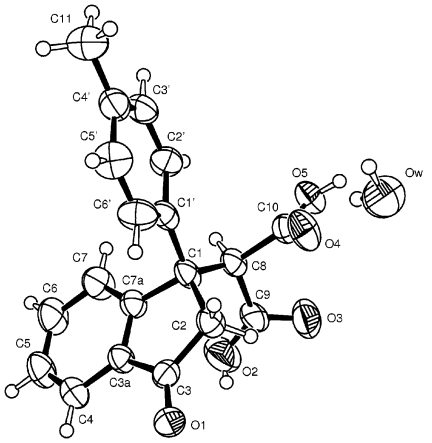

Figure 3. Crystal structure of the simplified analogue **21**−H_2O. Ellipsoids enclose 50% of probability.

concerning compounds **19** and **20** showed the surprising role of a second carboxyl group in the interaction of these stand alone indanone derivatives with the AT_1 receptor. Compounds **19** and **20** can be regarded as conformationally restrained derivatives of some diphenylpropionic acid derivatives described

Table 1. AT_1 Receptor Binding Affinities of Compounds **2**, **4**−**6**, **17**, **19**, and **20**

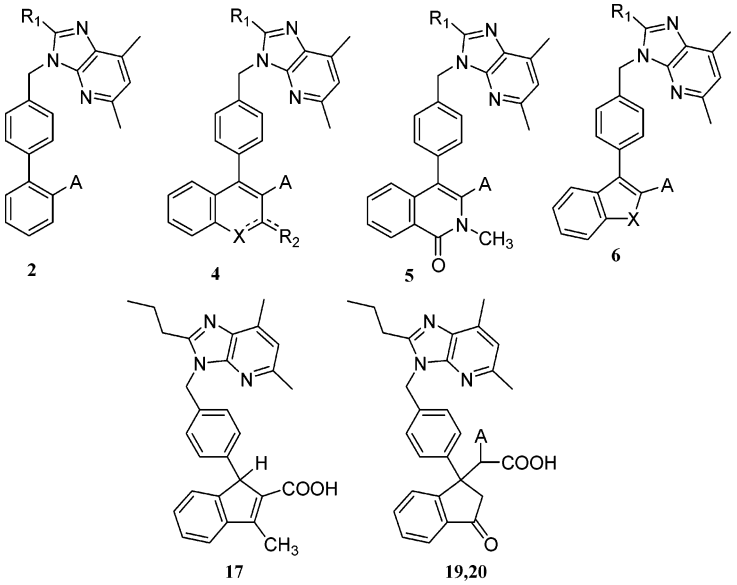

2 **4** **5** **6** **17** **19,20**

compd	X	R_1	R_2	A	binding IC_{50} (nM) ± SEM[a]	rabbit aortic strips IC_{50} (nM) ± SEM[b]
2a (L-158,809)		C_2H_5		CN_4H	0.4 ± 0.1	
2b		*n*-C_3H_7		CN_4H	0.8 ± 0.01	
2c		C_2H_5		COOH	10 ± 2.2	
4a	CH	C_2H_5	H	COOH	33 ± 4.7	
4b (CR3210)	N	C_2H_5	H	CN_4H	6.9 ± 1.3	8.9 ± 2.9 (4.0)
4c	N	C_2H_5	H	COOH	17 ± 1.8	
4d	N	C_2H_5	NH_2	COOH	13 ± 1.2	
4e	N-CH_3	C_2H_5	=O	CN_4H	>300	
4f	N-CH_3	C_2H_5	=O	COOH	326 ± 36	
4g	N	*n*-C_3H_7	H	CN_4H	12 ± 2.1	
4h	N	*n*-C_3H_7	H	COOH	11 ± 1.8	
4i	N	*n*-C_3H_7	Cl	COOH	7.7 ± 1.0	
4j	N	*n*-C_3H_7	CH_3	COOH	9.0 ± 1.6	(13)
4k	N	*n*-C_3H_7	NH_2	COOH	4.2 ± 0.34	(3.3)
4l	N	*n*-C_3H_7	H	$CONHSO_2C_6H_4(p)NO_2$	106 ± 19	
4m	N	*n*-C_4H_9	H	COOH	41 ± 7.1	
4n	N	*n*-C_4H_9	NH_2	COOH	13 ± 1.5	
5a		C_2H_5		CN_4H	>300	
5b (CR3588)		C_2H_5		COOH	5.2 ± 0.3	4.6 ± 0.9
5c		*n*-C_3H_7		CN_4H	>300	
5d		*n*-C_3H_7		COOH	5.7 ± 0.9	
5e		*n*-C_4H_9		CN_4H	>300	
5f		*n*-C_4H_9		COOH	6.2 ± 1.1	
6a	C=O	C_2H_5		COOH	53 ± 7.9	
6b	C=O	*n*-C_3H_7		COOH	50 ± 15	
6c	$C=CH_2$	*n*-C_3H_7		COOH	60 ± 17	
6d	$C(H)CH_3$	*n*-C_3H_7		COOH	99 ± 22	
6e	$C(OH)CH_3$	*n*-C_3H_7		COOH	11 ± 1.4	33 ± 6.4
6f	$C(OH)C_2H_5$	*n*-C_3H_7		COOH	15 ± 1.5	
6g	C=O	*n*-C_3H_7		$CONHSO_2CH_3$	54 ± 5.1	
6h	C=O	*n*-C_3H_7		$CONHSO_2C_6H_5$	131 ± 12	
17					47 ± 4.4	
19				H	139 ± 12	
20				COOH	55 ± 4.9	
Ang II					0.4 ± 0.1	
losartan					6.7 ± 0.5	10 ± 1.7 (9.9)
valsartan					1.9 ± 0.2	

[a] Each value is the mean ± SEM of three determinations and represents the concentration giving half the maximum inhibition of [^{125}I]Sar^1,Ile^8-Ang II specific binding to rat hepatic membranes. [b] The antagonism of Ang II-contracted rabbit aorta strips was assayed by using 60 min as time of contact of the tested compound. Only one antagonist concentration was tested on each tissue preparation. The values in parentheses are the ones described in a previous article (see ref 6).

in the literature, in which the monoacid shows the same affinity as that of the diacid derivative.[17]

(b) Effects of the Modification of the Acidic Moiety. It is noteworthy that in the series of isoquinolinone derivatives **5**, the replacement of the carboxyl moiety of compounds **5b**,**d**,**f** with the tetrazole group (compounds **5a**,**c**,**e**) produces a dramatic decrease in receptor affinity, whereas in the series of quinoline derivates **4b**,**c**,**g**,**h**, the two different acidic moieties appeared to be completely bioisoster.[6] However, we previously observed that in the series of monocyclic compounds **2**, the same

structural modification lead to an affinity enhancement of about 1 order of magnitude, and this effect was comparable with that reported in the literature for losartan.[18]

A comparison between acid **6b** and acylsulfonamide derivative **6g** suggests that an extended acidic group is tolerated in such compounds by the AT_1 receptor binding site, provided it is not excessively bulky. In fact, the replacement of the methylsulfonamido group of **6g** with the phenylsulfonamido group of **6h** produces a slight decrease in affinity as previously observed in a series of diphenylpropionic acid derivatives described in the literature.[17]

(c) Effects of the Modification of the Lipophilic Substituent in Position 2 of the Imidazo[4,5-*b*]pyridine Nucleus. We previously observed that ethyl derivative **2a** showed a 2-fold higher affinity with respect to propyl derivative **2b** in our test system, and a similar SAFIR trend was found for the couple of bicyclic tetrazole derivatives **4b** and **4g**.[6] However, a small deviation from this trend was observed in the case of the short series of carboxylic derivatives **4c**,**h**,**l**, where the optimal lipophilic substituent appeared to be the *n*-propyl group.[6] In the present series of compounds **5** and **6**, the variation of the lipophilic substituent in position 2 of the imidazo[4,5-*b*]pyridine nucleus has an even more negligible effect than that already observed in the other series.

Functional Studies. Three nanomolar affinity AT_1 receptor ligands (**5b**, **6e**, and the previously described **4b** as reference standard) were selected from the three structural subclasses of the AT_1 ligands described in the article, and their potential antagonistic activity was investigated in vitro, using the contractile response of isolated rabbit aortic strips as a functional assay. In control experiments, the response to Ang II (5 nM) that induced a submaximal contraction remained stable during the entire experimental period, and no tachyphylaxis was observed. However, compounds **4b**, **5b**, and **6e** were devoid of intrinsic activity and inhibited the response to Ang II showing IC_{50} values well related to their binding affinities (Table 1). Moreover, a significant reduction in the recovery of the contractile response was observed after the washout of antagonists **4b**, **5b**, and **6e**, providing evidence for an insurmountable antagonism.

Molecular Modeling Studies. To assess the prediction capability of previously generated chemical feature based pharmacophore models of AT_1 receptor antagonists,[10] a comparative study was performed, and the following results were obtained. All compounds with activity values in the subnanomolar range were identified by both a quantitative and a qualitative pharmacophore model presented earlier, Hypo1 (five feature pharmacophore model; seven points; one hydrophobic aromatic, one hydrophobic aliphatic, a hydrogen bond acceptor, a negative ionizable function, and an aromatic plane function) presented in Figure 4, and Hypo2 (seven feature pharmacophore; 11 points; two aromatic rings, two hydrogen bond acceptors, a negative ionizable function, and two hydrophobic functions) presented in Figure 7, respectively.[10] The mapping of the highest active compounds (compounds **2a** and **2b**) is shown for the two pharmacophore hypothesis in Figures 6 and 9. In the data set of 34 compounds reported in Table 1, 22 (65%) were retrieved by the fast search algorithm and 34 (100%) by the best search algorithm within the software Catalyst.[19] Five of the nine compounds with high inhibitory potency against the AT_1 receptor (i.e., 9 compounds show IC_{50} values higher than 10 nM) mapped on the pharmacophore pattern of Hypo1 are shown in Figure 5. The mapping of the two substances with subnanomolar activity (compounds **2a** and **2b**) against the AT_1 receptor is presented in Figure 6. The quantitative pharmacophore model (Hypo1) is able to detect almost the entire data set of compounds with inhibitory activity against the AT_1 receptor presented in this study. The qualitative pharmacophore model (Hypo2) was able to retrieve 23 of the 34 active AT_1 receptor antagonists in the fast flexible search procedure (68%) and 33 of the data set (34 compounds) in the best flexible search procedure (97%). The activity estimation of the quantitative pharmacophore model (Hypo1, Figure 4) yielded no satisfying results. Therefore, we tried to predict activities by the qualitative pharmacophore modeling approach. (Hypo 2, Figure 7) For this procedure, we submitted the compounds to a calculation of the best fit values. The fit value represents the mapping of chemical substructures into feature constraints, as well as the distance deviation of chemical functions from the center of the feature. Therefore, the geometric fit value points out exactly how the

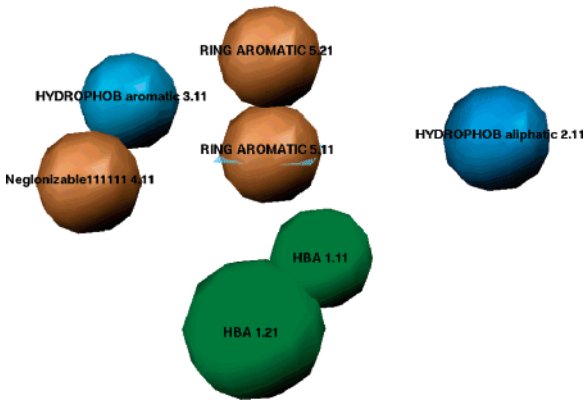

Figure 4. Quantitative pharmacophore model Hypo1.

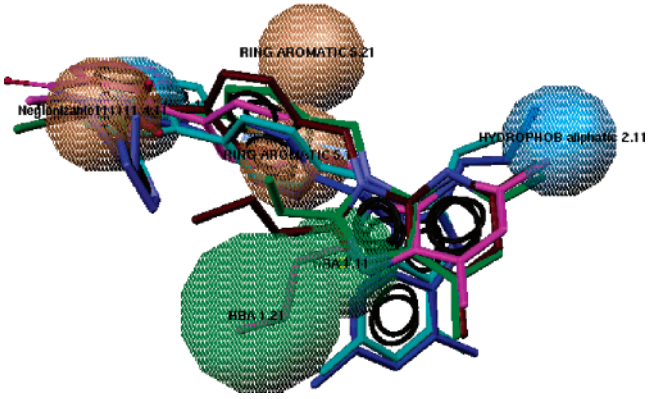

Figure 5. Mapping of highly active compounds (**2a**, **2b**, **4b**, **4i**, **5d**) to quantitative pharmacophore model Hypo1.

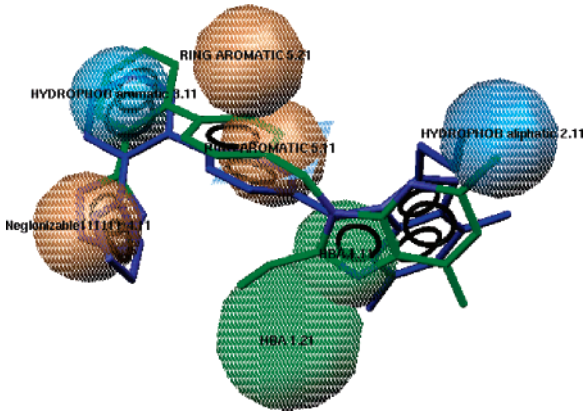

Figure 6. Mapping of compounds **2a** and **2b** to quantitative pharmacophore model Hypo1.

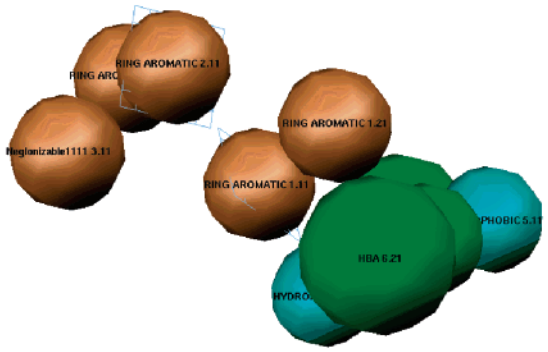

Figure 7. Representation of qualitative pharmacophore model Hypo2.

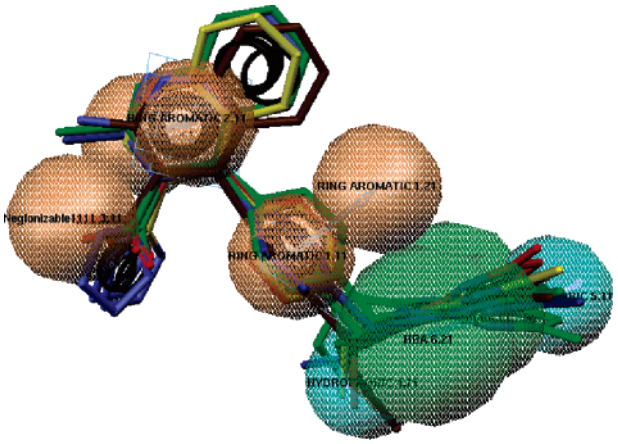

Figure 8. Representation of Hypo2 mapped to six highly active compounds (IC_{50} values lower than 10 nM: compounds **2a**, **2b**, **4b**, **4i**−**k**).

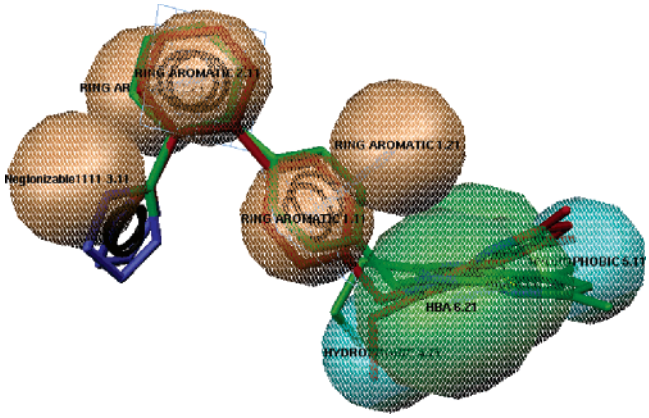

Figure 9. Mapping of compounds **2a** and **2b** to qualitative Hypo2.

function is localized at the center of a feature sphere. This value ranks the compounds according to their mapping goodness on a single pharmacophore model. In qualitative pharmacophore models, each feature makes a contribution to the fit value of one; hence, the Hypo2 can have a maximum fit value of seven (seven features). The qualitative pharmacophore model was able to retrieve 20 of the 26 substances (77%) with activity values up to 100 nM in the fast flexible search algorithm and 26 of the 26 substances (100%) using the best flexible search algorithm. A best fit threshold of 5 was used to distinguish between highly active and moderately active compounds. Under these considerations, 16 compounds with activity values up to 100 nM were found to be above this borderline. Hence, 16 of the 26 compounds (62%) were predicted by the pharmacophore model Hypo2, considering five a fit threshold value in the fast flexible search algorithm within the Catalyst software package. A qualitative predictive trend was also obvious in the comparison of the fit values and the measured activity data when only compounds with IC_{50} values of 10 nM or even higher were considered (nine compounds). Six of these nine molecules (67%) were retrieved by our seven chemical feature HipHop pharmacophore model (Hypo2), considering five a fit borderline value (Figure 8). Hence, only molecules with a fit value higher than five were considered in this approach. The qualitative pharmacophore model (Hypo2) is able to discriminate between highly active and moderately active compounds in about two-thirds of the experimented cases. Enrichment can accelerate the time of detection of new active compounds in the lead identification phase. In summary, 6 of the nine highly active compounds (i.e., IC_{50} higher than 10 nM) and 16 of the 26 moderately active compounds (IC_{50} values up to 100 nM) were predicted correctly by the pharmacophore model Hypo2, considering the borderline of a fit value higher than five. The two compounds with the highest activity values are mapped onto pharmacophore model Hypo2 in Figure 9.

Intestinal Permeability Experiments in Vitro. Permeability studies performed with Caco-2 monolayers[20] show that quinoline derivative **4b** and isoquinolinones **5b**,**f** are chemical entities characterized by a very low permeability in apical to basolateral experiments (P_{app} values ranging from 0.10 to 0.01 $\times$ 10^{-6} cm/s, Table 2). For comparison, propanolol (90% absorbed in humans) showed a P_{app} value of 30.5 $\times$ 10^{-6} cm/s in the same test and vinblastine (a well-known P-glycoprotein substrate) a P_{app} value of 0.08 $\times$ 10^{-6} cm/s. In the short series of compounds evaluated in such a test system, the most permeable was 3-tetrazolylquinoline derivative **4b**, which showed a P_{app} value very similar to that shown by vinblastine and was about 1 order of magnitude more permeable than isoquinolinone derivative **5f**. It is noteworthy that the decreased lipophilicity of ethyl derivative **5b** with respect to butyl derivative **5f** is linked to a slightly higher permeability.

Pharmacokinetic Studies. The pharmacokinetic properties of compounds **4b** (CR3210), **4i**,**j**,**k**, and **5b** (CR3588) were evaluated in rats by standard procedures[7,8] in comparison with reference AT_1 antagonist **1** (losartan). The results shown in Table 2 suggest that compounds **4b**,**i**,**j**,**k**, and **5b** are barely bioavailable chemical entities characterized by a poor intestinal absorption and a rapid excretion. As expected, there is a positive correlation between the oral bioavailability and the Caco-2 permeability values of compounds **4b** and **5b**.[20b] In fact, 3-tetrazolylquinoline derivative **4d**, which showed a P_{app} value of 0.10 $\times$ 10^{-6} cm/s showed a bioavailability of 49%, whereas isoquinolinone derivative **5b**, which showed a P_{app} value of 0.03 $\times$ 10^{-6} cm/s was not bioavailable at all.

Discussion

The starting point of our research program, focused on the development of new AT_1 receptor antagonists as antihypertensive agents, was 4-phenyl-3-tetrazolylpyridine derivative **2d**, which was described both to show an affinity four times lower than its carbaisoster **2c** and to be an orally active Ang II antagonist showing a poorer oral bioavailability (probably for the decreased lipophilicity) than that of **2c**.[5] Our working hypothesis concerned the introduction of a fused benzene ring into the tetrazolylpyridyl derivative **2d** structure in order to ensure the lipophilicity necessary for good oral bioavailability. The first step of the work led to the discovery of a series of quinoline derivatives **4** showing in vitro properties comparable to those shown by losartan. Investigations on the biopharmaceutical properties of the selected candidate for further pre-

Table 2. Pharmacokinetic Parameters of Compounds **1**, **2a**, **4b**,**i**,**j**,**k**, and **5b**,**f**

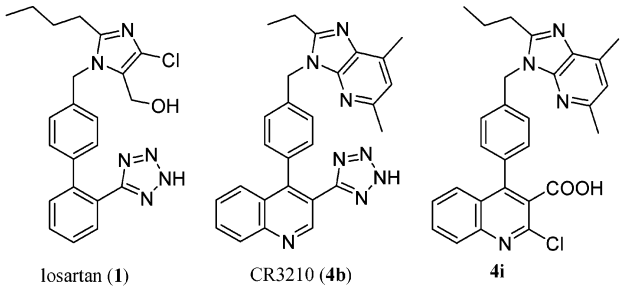

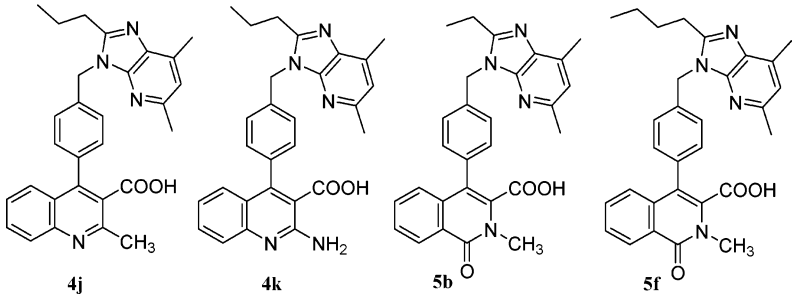

compd	MW	*C* log *P*[a]	Caco-2 permeability P_{app} (a−b)[b] ($\times 10^{-6}$ cm/s)	dose (mg/kg) (route)	AUC (μg·h/mL)	$t_{1/2}$[c] (h)	C_{max}[d] (μg/mL)	t_{max}[e] (h)	oral bioavail. (%)
4b (CR3210)	460.53	4.7	0.10	3 (iv)	0.89	0.68			
				30 (os)	4.4	1.0	4.2	0.5	49
4i	484.98	5.8		3 (iv)	0.34	0.30			
4j	464.56	5.8		3 (iv)	0.50	0.33			
4k	465.55	5.6		3 (iv)	0.52	0.28			
5b (CR3588)	466.53	4.3	0.03	3 (iv)	0.63	0.22			0
				10 (os)	0				
5f	494.58	5.3	0.01						
1 (losartan)	422.91	4.1[f]	1.15[g]	3 (iv)	12.4	4.7			
				30 (os)	74.8	3.0	27.5	0.5	60

[a] *C* log *P* calculated by means of CS ChemDraw Ultra 8.0 (Cambridge Soft Corporation, Cambridge, MA 02140). [b] Apical to basolateral Caco-2 permeability. [c] $t_{1/2}$: terminal half-life. [d] C_{max}: observed maximum concentration after administration. [e] t_{max}: time to reach maximum concentration. [f] For comparison, the log P_{HPLC} value described in the literature was 4.2; see ref 21. [g] See ref 21.

clinical studies (CR3210, **4b**) revealed a rather complex picture from which the low permeability, the relatively low oral bioavailability (49%, Table 2), the rapid excretion ($t_{1/2}$ = 0.68−1.0 h),[8] and the fast conjugation with glucuronic acid were clearly demonstrated.[22] Therefore, the transformation of the distal phenyl ring of L-158,809 (or the pyridine one of **2d**) into the quinoline nucleus of **4b** was tolerated at the receptor level, but it was deleterious for pharmacokinetic properties. In other words, our hypothesis on the importance of lipophilicity for oral bioavailability and, more in general, for suitability of suitable pharmacokinetic properties was not correct in the case of this class of AT$_1$ receptor antagonists. Because the main difference between **4b** (CR3210) and **2a** (L-158,809) appeared to be the higher effectiveness of the conjugation of **4b** with glucuronic acid,[22] the design of the new AT$_1$ receptor antagonists should appropriately consider the interaction of the UDP-glucuronosyltransferases (EC 2.4.1.17) because these appear to play a key role in the metabolism (and excretion) of tetrazole derivatives.[23] Moreover, the pharmacokinetic studies performed on other quinoline derivatives selected on the basis of their in vitro potency (compounds **4i**,**j**,**k**) showed very rapid excretion ($t_{1/2}$ values in the range from 0.22 to 0.33 h). Because small structural modifications could affect the interaction with hepatic transporters and/or with UDP-glucuronosyltransferases in a significant way, both isoquinolinone derivatives **5** and indene derivatives **6** were designed and synthesized.

Interestingly, the SAFIR obtained with the newly synthesized compounds showed that the isoquinolinone moiety of compounds **5b**,**d**,**f** is better (from the point of view of the interaction with the AT$_1$ receptor) than benzene, naphthalene, and quinoline of compounds **2** and **4**. The isoquinolinone moiety looks like a molecular fragment optimized for the interaction with the top of the AT$_1$ receptor binding cavity, but it appears to be incompatible with the presence of the tetrazole moiety because the tetrazolyl derivatives **5a**,**c**,**e** were found (to our surprise) to be inactive. Owing to the in vitro potency of carboxylic acids **5b**,**d**,**f**, their evaluation in pharmacokinetic studies was performed showing that the bioavailability problems of compound **5b** are probably related to its very low permeability (P_{app} (a−b) = 0.03 $\times$ 10^{-6} cm/s).[20b]

As a final step of the work, we explored the chemistry and the structure−affinity relationships of indene derivatives **6**. The results of the binding studies performed on compounds **6** were not very exciting, because the first members of this subclass (**6a**,**b**) proved to be 1 order of magnitude less potent than isoquinolinones **5b**,**d**,**f**, and only after meticulous optimization work, we were able to obtain compounds **6e**,**f** provided with more interesting AT$_1$ receptor affinity. The optimization also produced interesting SAFIR data, which provided information on the binding site topology and above all a polymerizing AT$_1$ receptor ligand (**6c**). This bioactive monomer formed a thermoreversible polymer (poly-**6c**) and was released from the latter

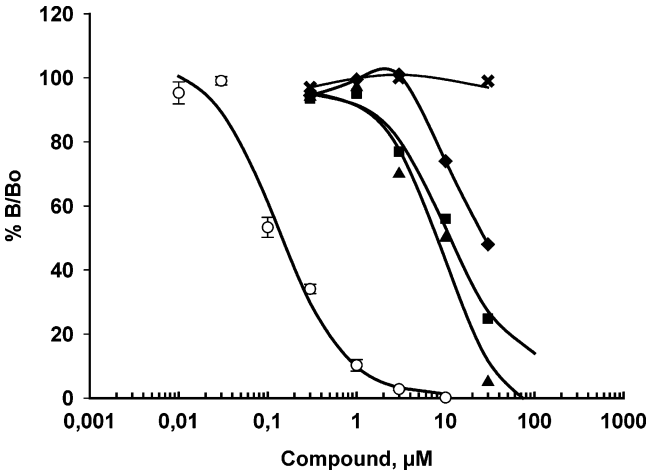

Figure 10. Competition curves of poly-**6c**, its monomer **6c**, and PTSA obtained in AT_1 receptor binding studies. Stock solutions of **6c** and poly-**6c** (see Biological Methods section for details) were freshly prepared and then stored at 37 °C for 3 or 6 days. PTSA (×) was assayed because of its presence as an impurity of poly-**6c** and was revealed to be inactive. The assays performed on freshly prepared solutions of poly-**6c** (◆) revealed the presence of a detectable dose-dependent inhibition of the radioligand specific binding to AT_1 receptors. The inhibition curve of poly-**6c** is significantly shifted to the left because of the use of a stock solution stored in buffer at 37 °C for the first 3 days (■), but it did not change because of being stored for an additional 3 days (▲). On the contrary, monomer **6c**, tested in parallel in each assay, was insensitive to the storage conditions; values (○) indicated in the Figure are the mean ± standard error of three replicates.

with temperature-dependent kinetics until the establishment of a temperature-dependent equilibrium as it occurs in equilibrium polymerization processes (in these phenomena, the equilibrium monomer concentration is temperature-dependent).[24] Preliminary binding studies performed on poly-**6c** suggested that a detectable depolymerization occurred in buffer (pH 7.4) at room temperature, it increased its extent after a storage of the polymer solution at 37 °C and appeared to reach equilibrium within about 3 days at 37 °C (Figure 10). Interestingly, the apparent IC_{50} of poly-**6c** determined at the polymerization equilibrium appeared to be about 2 orders of magnitude higher than that shown by monomer **6c**. This result suggests that in these conditions poly-**6c** released one molecule of monomer **6c** each about 100 monomeric units. Further studies are in progress to define with precision the physicochemical constants of this equilibrium polymerization phenomenon and to explore the potentiality of this mechanism in drug controlled release from new polymeric prodrugs.

Finally, 34 compounds belonging to these structural subclasses of AT_1 receptor antagonists (**4**,**5**, and **6**) were used as a new test to evaluate the predictive capability of the previously published qualitative and quantitative pharmacophore models.[10,25] The results obtained in the validation of these models suggest that they can be used to evaluate new virtual libraries of potential AT_1 receptor antagonists in order to discover novel leads.

Experimental Section

Chemistry. All chemicals used were of reagent grade. Yields refer to purified products and are not optimized. Melting points were determined in open capillaries on a Gallenkamp apparatus and are uncorrected. Microanalyses were carried out by means of a Perkin-Elmer 240C or a Perkin-Elmer Series II CHNS/O Analyzer 2400. Merck silica gel 60 (230−400 mesh) was used for column chromatography. Merck TLC plates, silica gel 60 F_{254} were used for TLC. ^{1}H NMR spectra were recorded with a Bruker AC 200 spectrometer in the indicated solvents (TMS as the internal standard): the values of the chemical shifts are expressed in ppm and the coupling constants (*J*) in Hz. Mass spectra were recorded on either a Varian Saturn 3 spectrometer or a ThermoFinnigan LCQ-Deca.

General Procedure for the Preparation of Compounds 11a−f and 15a,b (Radical Bromination-Coupling Procedure). A mixture of the toluene derivative **10**, **13**, and **14** in 40 mL of CCl_4 with *N*-bromosuccinimide (1.02 equiv) and dibenzoyl peroxide (0.1 equiv) was refluxed for a suitable time (typically 2−3 h), and the reaction progress was monitored by TLC. The initial solvent volume was reduced by half under reduced pressure, the insoluble succinimide was filtered-off, and the resulting mixture was evaporated under reduced pressure. The residue was dissolved into anhydrous DMF (10 mL) and added to a mixture (aged at 0 °C for 20 min) of the appropriate 2-alkyl-5,7-dimethyl-3*H*-imidazo[4,5-*b*]pyridine[1] (1.0 equivalent) in anhydrous DMF (10 mL) with NaH (1.0 equivalent). The resulting mixture was stirred at room temperature for 15−18 h under argon, and the reaction was quenched with ice−water (5 mL). The bulk of the DMF was evaporated under reduced pressure, and the residue was diluted with water (20 mL) and extracted with ethyl acetate. The combined organic extracts were washed with brine, dried over sodium sulfate and concentrated under reduced pressure. Purification of the residue by flash chromatography with ethyl acetate-petroleum ether (7:3) (or ethyl acetate) as the eluent gave pure compounds **11a−f** and **15a**,**b**.

Ethyl 1,2-Dihydro-4-[4-[(5,7-dimethyl-2-ethyl-3*H*-imidazo[4,5-*b*]pyridin-3-yl)methyl]phenyl]-2-methyl-1-oxo-3-isoquinolinecarboxylate (11b). The title compound was prepared in 36% yield (0.33 g, mp 152−155 °C) starting from **10** (0.60 g, 1.87 mmol) and 5,7-dimethyl-2-ethyl-3*H*-imidazo[4,5-*b*]pyridine (0.33 g, 1.9 mmol) according to the general procedure for radical bromination and coupling. ^{1}H NMR ($CDCl_3$): 0.87 (t, J = 7.1, 3H), 1.34 (t, J = 7.6, 3H), 2.59 (s, 3H), 2.63 (s, 3H), 2.84 (q, J = 7.6, 2H), 3.57 (s, 3H), 3.97 (q, J = 7.1, 2H), 5.51 (s, 2H), 6.90 (s, 1H), 7.18−7.27 (m, 5H), 7.47−7.56 (m, 2H), 8.45−8.50 (m, 1H). MS(ESI) *m*/*z* 495 ($M + H^+$).

Ethyl 1,2-Dihydro-4-[4-[(5,7-dimethyl-2-propyl-3*H*-imidazo[4,5-b]pyridin-3-yl)methyl]phenyl]-2-methyl-1-oxo-3-isoquinolinecarboxylate (11d). The title compound was prepared in 32% yield (0.10 g) starting from **10** (0.20 g, 0.62 mmol) and 5,7-dimethyl-2-propyl-3*H*-imidazo[4,5-*b*]pyridine (0.12 g, 0.63 mmol) according to the general procedure for radical bromination and coupling. ^{1}H NMR ($CDCl_3$): 0.86 (t, J = 7.3, 3H), 0.97 (t, J = 7.3, 3H), 1.68−1.85 (m, 2H), 2.57 (s, 3H), 2.61 (s, 3H), 2.79 (t, J = 7.6, 2H), 3.56 (s, 3H), 3.96 (q, J = 7.3, 2H), 5.50 (s, 2H), 6.88 (s, 1H), 7.17−7.26 (m, 5H), 7.47−7.51 (m, 2H), 8.43−8.48 (m, 1H).

Ethyl 1,2-Dihydro-4-[4-[(2-butyl-5,7-dimethyl-3*H*-imidazo[4,5-*b*]pyridin-3-yl)methyl]phenyl]-2-methyl-1-oxo-3-isoquinolinecarboxylate (11f). The title compound was prepared in 34% yield (0.14 g) starting from **10** (0.25 g, 0.78 mmol) and 2-butyl-5,7-dimethyl-3*H*-imidazo[4,5-*b*]pyridine (0.16 g, 0.79 mmol) according to the general procedure for radical bromination and coupling. ^{1}H NMR ($CDCl_3$): 0.86−0.96 (m, 6H), 1.32−1.51 (m, 2H), 1.67−1.82 (m, 2H), 2.60 (s, 3H), 2.64 (s, 3H), 2.81 (t, J = 7.9, 2H), 3.59 (s, 3H), 3.99 (q, J = 7.2, 2H), 5.52 (s, 2H), 6.91 (s, 1H), 6.90−7.14 (m, 1H), 7.19−7.25 (m, 4H), 7.50−7.54 (m, 2H), 8.47−8.51 (m, 1H). MS(ESI) *m*/*z* 523 ($M + H^+$).

4-[4-[(5,7-Dimethyl-2-ethyl-3*H*-imidazo[4,5-*b*]pyridin-3-yl)-methyl]phenyl]-2-methyl-3-[2-(triphenylmethyl)-2*H*-tetrazol-5-yl]-1(2*H*)-isoquinolinone (11a). The title compound was prepared in 45% yield (0.070 g, mp 174−180 °C) starting from **13** (0.12 g, 0.21 mmol) and 5,7-dimethyl-2-ethyl-3*H*-imidazo[4,5-*b*]pyridine (0.040 g, 0.23 mmol) according to the general procedure for radical bromination and coupling. ^{1}H NMR ($CDCl_3$): 1.25 (t, J = 7.6, 3H), 2.58 (s, 3H), 2.66 (s, 3H), 2.71 (q, J = 7.6, 2H), 3.30 (s, 3H), 5.42 (s, 2H), 6.88−6.93 (m, 7H), 7.04−7.15 (m, 4H), 7.21−7.34 (m, 10H), 7.51−7.56 (m, 2H), 8.49−8.58 (m, 1H). MS(ESI) *m*/*z* 733 ($M + H^+$).

4-[4-[(5,7-Dimethyl-2-propyl-3*H*-imidazo[4,5-*b*]pyridin-3-yl)-methyl]phenyl]-2-methyl-3-[2-(triphenylmethyl)-2*H*-tetrazol-5-yl]-1(2*H*)-isoquinolinone (11c). The title compound was prepared in 41% yield (0.065 g, mp 170−174 °C) starting from **13** (0.12 g, 0.21 mmol) and 5,7-dimethyl-2-propyl-3*H*-imidazo[4,5-*b*]pyridine (0.04 g, 0.21 mmol) according to the general procedure for radical bromination and coupling. ^{1}H NMR ($CDCl_3$): 0.90 (t, J = 7.3, 3H), 1.57−1.73 (m, 2H), 2.58 (s, 3H), 2.64−2.71 (m, 5H), 3.29 (s, 3H), 5.42 (s, 2H), 6.88−6.91 (m, 7H), 7.04−7.14 (m, 4H), 7.21−7.37 (m, 10H), 7.51−7.55 (m, 2H), 8.50−8.57 (m, 1H). MS(ESI) m/z 747 (M + H$^+$).

4-[4-[(2-Butyl-5,7-dimethyl-3*H*-imidazo[4,5-*b*]pyridin-3-yl)-methyl]phenyl]-2-methyl-3-[2-(triphenylmethyl)-2*H*-tetrazol-5-yl]-1(2*H*)-isoquinolinone (11e). The title compound was prepared in 74% yield (0.13 g, mp 160−162 °C) starting from **13** (0.13 g, 0.23 mmol) and 5,7-dimethyl-2-butyl-3*H*-imidazo[4,5-*b*]pyridine (0.050 g, 0.25 mmol) according to the general procedure for radical bromination and coupling. ^{1}H NMR ($CDCl_3$): 0.86 (t, J = 7.1, 3H), 1.21−1.41 (m, 2H), 1.54−1.70 (m, 2H), 2.58 (s, 3H), 2.64 (s, 3H), 2.70 (t, J = 7.6, 2H), 3.29 (s, 3H), 5.41 (s, 2H), 6.88−6.91 (m, 7H), 7.04−7.14 (m, 4H), 7.22−7.38 (m, 10H), 7.50−7.57 (m, 2H), 8.50−8.55 (m, 1H). MS(ESI) m/z 761 (M + H$^+$).

***tert*-Butyl 3-[4-[(5,7-Dimethyl-2-ethyl-3*H*-imidazo[4,5-*b*]pyridin-3-yl)methyl]phenyl]-1-oxo-1*H*-indene-2-carboxylate (15a).** The title compound was prepared in 33% yield (0.10 g of yellow solid melting at 119−123 °C) starting from **14** (0.20 g, 0.62 mmol) and 5,7-dimethyl-2-ethyl-3*H*-imidazo[4,5-*b*]pyridine (0.11 g, 0.63 mmol) according to the general procedure for radical bromination and coupling. ^{1}H NMR ($CDCl_3$): 1.32 (t, J = 7.4, 3H), 1.29 (s, 9H), 2.56 (s, 3H), 2.61 (s, 3H), 2.78 (q, J = 7.4, 2H), 5.51 (s, 2H), 6.88 (s, 1H), 7.04 (m, 1H), 7.23 (d, J = 8.1, 2H), 7.33 (m, 2H), 7.41 (d, J = 8.1, 2H), 7.53 (m, 1H). MS(ESI) m/z 494 (M + H$^+$).

***tert*-Butyl 3-[4-[(5,7-Dimethyl-2-propyl-3*H*-imidazo[4,5-*b*]pyridin-3-yl)methyl]phenyl]-1-oxo-1*H*-indene-2-carboxylate (15b).** The title compound was prepared in 46% yield (0.80 g of yellow glassy solid) starting from **14** (1.1 g, 3.4 mmol) and 5,7-dimethyl-2-propyl-3*H*-imidazo[4,5-*b*]pyridine (0.67 g, 3.5 mmol) according to the general procedure for radical bromination and coupling.^{1}H NMR ($CDCl_3$): 0.97 (t, J = 7.4, 3H), 1.31 (s, 9H), 1.69−1.88 (m, 2H), 2.58 (s, 3H), 2.62 (s, 3H), 2.77 (t, J = 7.7, 2H), 5.53 (s, 2H), 6.90 (s, 1H), 7.06 (m, 1H), 7.24 (d, J = 8.3, 2H), 7.34 (m, 2H), 7.42 (d, J = 8.3, 2H), 7.53 (m, 1H). MS(ESI) m/z 508 (M + H$^+$).

Preparation of Target Carboxylic Acid Derivatives 5b,d,f (Basic Hydrolysis). To a solution of the appropriate ester (**11b**,**d**,**f**) (0.2−0.6 mmol) in ethanol (20 mL), 2 N NaOH (2.0 mL) was added, and the resulting mixture was refluxed while the reaction progress was monitored by TLC. When the ester derivative disappeared from the chromatogram, the reaction mixture was evaporated under reduced pressure and diluted with water (20 mL), and the pH was adjusted to 5−6 by the addition of 1 N HCl. The precipitate was collected by filtration (or extracted with chloroform when necessary), washed with water, and dried under reduced pressure. Purification of the solid obtained by washing with ethyl acetate or diethyl ether gave the pure target carboxylic acid derivatives.

1,2-Dihydro-4-[4-[(5,7-dimethyl-2-ethyl-3*H*-imidazo[4,5-*b*]pyridin-3-yl)methyl]phenyl]-2-methyl-1-oxo-3-isoquinolinecarboxylic Acid (5b). This compound was prepared in 83% yield (0.22 g, white solid, mp >300 °C) starting from the ethyl ester **11b** (0.28 g, 0.57 mmol) according to the general procedure for basic hydrolysis. ^{1}H NMR ($CDCl_3$): 1.38 (t, J = 7.6, 3H), 2.61 (s, 6H), 2.88 (q, J = 7.6, 2H), 3.69 (s, 3H), 5.46 (s, 2H), 6.88 (s, 1H), 7.05 (d, J = 8.1, 1H), 7.19 (d, J = 8.1, 2H), 7.32−7.47 (m, 4H), 8.42−8.45 (m, 1H). MS(ESI negative ions) m/z 465 (M − H$^+$). Anal. ($C_{28}H_{26}N_4O_3\cdot H_2O$) C,H,N.

1,2-Dihydro-4-[4-[(5,7-dimethyl-2-propyl-3*H*-imidazo[4,5-*b*]-pyridin-3-yl)methyl]phenyl]-2-methyl-1-oxo-3-isoquinolinecarboxylic Acid (5d). This compound was prepared in 83% yield (0.080 g, mp >300 °C) starting from ethyl ester **11d** (0.10 g, 0.20 mmol) according to the general procedure for basic hydrolysis. ^{1}H NMR ($CDCl_3$): 0.91 (t, J = 7.5, 3H), 1.74−1.89 (m, 2H), 2.59 (s, 6H), 2.83 (t, J = 7.7, 2H), 3.70 (s, 3H), 5.47 (s, 2H), 6.88 (s, 1H), 7.05 (d, J = 7.7, 1H), 7.19 (d, J = 8.1, 2H), 7.32−7.47 (m, 4H), 8.42−8.45 (m, 1H). MS(ESI negative ions) m/z 479 (M − H$^+$). Anal. ($C_{29}H_{28}N_4O_3\cdot 0.5\ H_2O$) C,H,N.

1,2-Dihydro-4-[4-[(2-butyl-5,7-dimethyl-3*H*-imidazo[4,5-*b*]pyridin-3-yl)methyl]phenyl]-2-methyl-1-oxo-3-isoquinolinecarboxylic Acid (5f). This compound was prepared in 79% yield (0.090 g, mp 292−295 °C) starting from ethyl ester **11f** (0.12 g, 0.23 mmol) according to the general procedure for the basic hydrolysis. ^{1}H NMR ($CDCl_3$): 0.70 (t, J = 7.1, 3H), 1.03−1.14 (m, 2H), 1.32−1.40 (m, 2H), 2.58−2.69 (m, 8H), 3.74 (s, 3H), 5.53 (s, 2H), 7.00 (s, 1H), 7.08−7.12 (m, 1H), 7.22 (d, J = 8.0, 2H), 7.41−7.55 (m, 4H), 8.48−8.52 (m, 1H). MS(ESI negative ions) m/z 493 (M − H$^+$). Anal. ($C_{30}H_{30}N_4O_3\cdot 0.5\ H_2O$) C,H,N.

Preparation of Target Tetrazole Derivatives 5a,c,e (Deprotection of the Trityl-Protected Tetrazole Derivatives). A mixture of the appropriate trityl-protected tetrazole derivative (0.4−0.6 mmol) with formic acid (15 mL) was stirred at room temperature under argon for a suitable time (18−48 h), and the reaction progress was monitored by TLC. When the trityl-protected tetrazole derivative disappeared from the chromatogram, the reaction mixture was evaporated under reduced pressure. Purification of the residue by washing with diethyl ether or ethyl acetate gave the pure target compounds.

4-[4-[(5,7-Dimethyl-2-ethyl-3*H*-imidazo[4,5-*b*]pyridin-3-yl)-methyl]phenyl]-2-methyl-3-(2*H*-tetrazol-5-yl)-1(2*H*)-isoquinolinone (5a). This compound was prepared in 68% yield (0.020 g of white solid melting at 194−198 °C) starting from the protected tetrazolyl derivate **11a** (0.044 g, 0.060 mmol) according to the general procedure for acid hydrolysis. ^{1}H NMR ($CDCl_3$): 0.95 (br t, 3H), 2.59 (s, 3H), 2.63 (s, 3H), 2.85 (br q, 2H), 3.30 (s, 3H), 3.98 (br s, H$^+$ + H_2O), 5.52 (s, 2H), 7.02−7.06 (m, 3H), 7.13−7.20 (m, 3H), 7.53−7.57 (m, 2H), 8.52−8.57 (m, 1H). MS(ESI) m/z 491 (M + H$^+$). Anal. ($C_{28}H_{26}N_8O\cdot 2\ H_2O$) C,H,N.

4-[4-[(5,7-Dimethyl-2-propyl-3*H*-imidazo[4,5-*b*]pyridin-3-yl)-methyl]phenyl]-2-methyl-3-(2*H*-tetrazol-5-yl)-1(2*H*)-isoquinolinone (5c). This compound was prepared in 73% yield (0.022 g of white solid melting at 174−179 °C) starting from protected tetrazolyl derivate **11c** (0.045 g, 0.060 mmol) according to the general procedure for acid hydrolysis. ^{1}H NMR ($CDCl_3$): 0.77 (br t, 3H), 1.40−1.60 (br m, 2H), 2.64 (s, 6H), 2.86 (br t, 2H), 3.29 (s, 3H), 3.50 (br s, H$^+$ + H_2O), 5.53 (s, 2H), 7.02−7.28 (m, 6H), 7.49−7.75 (m, 2H), 8.49−8.64 (m, 1H). MS(ESI) m/z 505 (M + H$^+$). Anal. ($C_{29}H_{28}N_8O\cdot H_2O$) C,H,N.

4-[4-[(2-Butyl-5,7-dimethyl-3*H*-imidazo[4,5-*b*]pyridin-3-yl)-methyl]phenyl]-2-methyl-3-(2*H*-tetrazol-5-yl)-1(2*H*)-isoquinolinone (5e). This compound was prepared in 98% yield (0.023 g of white solid melting at 169−173 °C) starting from protected tetrazolyl derivate **11e** (0.034 g, 0.045 mmol) according to the general procedure for acid hydrolysis. ^{1}H NMR ($CDCl_3$, TEA): 0.88 (t, J = 7.2, 3H), 1.30−1.41 (m, 2H), 1.56−1.71 (m, 2H), 2.55 (s, 3H), 2.59 (s, 3H), 2.75 (t, J = 7.3, 2H), 3.28 (s, 3H), 4.30 (br s, H$^+$ + H_2O), 5.33 (s, 2H), 6.86 (s, 1H), 6.96 (d, J = 7.9, 2H), 7.08−7.15 (m, 3H), 7.45−7.49 (m, 2H), 8.49−8.54 (m, 1H). MS(ESI) m/z 519 (M + H$^+$). Anal. ($C_{30}H_{30}N_8O\cdot 0.5\ H_2O$) C,H,N.

Preparation of Target Carboxylic Acid Derivatives 6a,b,e,f (Acid Hydrolysis). A mixture of the suitable ester (0.1−0.39 mmol) with formic acid (15 mL) was stirred at room temperature under argon for a suitable time (typically 18h), and the reaction progress was monitored by TLC. When the ester disappeared from the chromatogram, the reaction mixture was evaporated under reduced pressure. Purification of the residue by washing with diethyl ether gave the pure target compounds.

3-[4-[(5,7-Dimethyl-2-ethyl-3*H*-imidazo[4,5-*b*]pyridin-3-yl)-methyl]phenyl]-1-oxo-1*H*-indene-2-carboxylic Acid (6a). This compound was prepared in 80% yield (0.035 g of yellow solid melting at 197−198 °C) starting from the *tert*-butyl ester 15a (0.050 g, 0.10 mmol) according to the general procedure for acid hydrolysis. ^{1}H NMR ($CDCl_3$): 1.31 (t, J = 7.5, 3H), 2.58 (s, 3H), 2.62 (s, 3H), 2.71 (q, J = 7.5, 2H), 5.53 (s, 2H), 6.90 (s, 1H), 7.16

(m, 1H), 7.26 (d, $J = 8.4$, 2H), 7.44 (m, 2H), 7.60 (m, 3H). MS-(ESI negative ions) *m/z* 436 ($M - H^+$). Anal. ($C_{27}H_{23}N_3O_3 \cdot 0.33\ H_2O$) C,H,N.

3-[4-[(5,7-Dimethyl-2-propyl-3*H*-imidazo[4,5-*b*]pyridin-3-yl)-methyl]phenyl]-1-oxo-1*H*-indene-2-carboxylic Acid (6b). This compound was prepared in 91% yield (0.16 g of yellow solid melting at 209−213 °C) starting from *tert*-butyl ester **15b** (0.20 g, 0.39 mmol) according to the general procedure for acid hydrolysis. ^{1}H NMR ($CDCl_3$): 0.94 (t, $J = 7.3$, 3H), 1.66−1.85 (m, 2H), 2.58 (s, 3H), 2.62 (s, 3H), 2.78 (t, $J = 7.7$, 2H), 5.54 (s, 2H), 6.90 (s, 1H), 7.17 (m, 1H), 7.26 (d, $J = 8.4$, 2H), 7.44 (m, 2H), 7.61 (m, 3H). MS(ESI negative ions) *m/z* 450 ($M - H^+$). Anal. ($C_{28}H_{25}N_3O_3 \cdot 0.5\ H_2O$) C,H,N.

3-[4-[(5,7-Dimethyl-2-propyl-3*H*-imidazo[4,5-*b*]pyridin-3-yl)-methyl]phenyl]-1-hydroxy-1-methyl-1*H*-indene-2-carboxylic Acid (6e). This compound was prepared from *tert*-butyl ester **16e** (0.15 g, 0.29 mmol) according to the general procedure for acid hydrolysis (reaction time 45 min) and was purified by washing with ether to give 0.045 g (yield 33%) of **6e** as a white solid (mp 246−247 °C). ^{1}H NMR (DMSO-d_6): 0.88 (t, $J = 7.3$, 3H), 1.58−1.70 (m, 5H), 2.49 (s, 6H), 2.74 (t, $J = 7.5$, 2H), 5.27 (br s, 1H), 5.50 (s, 2H), 6.96 (m, 2H), 7.13−7.38 (m, 6H), 7.47 (d, $J = 7.2$, 1H), 12.20 (br s, 1H). MS (ESI): *m/z* 468 ($M + H^+$). Anal. ($C_{29}H_{29}N_3O_3 \cdot 0.33\ H_2O$) C,H,N.

3-[4-[(5,7-Dimethyl-2-propyl-3*H*-imidazo[4,5-*b*]pyridin-3-yl)-methyl]phenyl]-1-ethyl-1-hydroxy-1*H*-indene-2-carboxylic Acid (6f). This compound was prepared from *tert*-butyl ester **16f** (0.030 g, 0.056 mmol) according to the general procedure for acid hydrolysis (reaction time 45 min) and was purified by washing with ether to obtain 0.011 g, mp 232−234 °C (yield 41%). ^{1}H NMR (DMSO-d_6): 0.41 (t, $J = 7.3$, 3H), 0.88 (t, $J = 7.3$, 3H), 1.58−1.77 (m, 2H), 1.98−2.07 (m, 1H), 2.28−2.38 (m, 1H), 2.49 (s, 6H), 2.74 (t, $J = 7.6$, 2H), 5.50 (s, 2H), 6.94 (m, 2H), 7.15−7.43 (m, 7H), 12.10 (br s, 1H). MS (ESI negative ions): *m/z* 480 ($M - H^+$). Anal. ($C_{30}H_{31}N_3O_3 \cdot 1.5\ H_2O$) C,H,N.

X-ray Crystallography. Single crystals of **19**·0.5 $CH_3COOC_2H_5$ and **21**·H_2O were submitted for X-ray data collection on a Siemens P4 four-circle diffractometer with graphite monochromated Mo−Kα radiation ($\lambda = 0.71069$ Å). The $\omega/2\theta$ scan technique was used for data collection.

The two structures were solved by direct methods implemented in the SHELXS-97 program.[26] The refinements were carried out by full-matrix anisotropic least-squares on F^2 for all reflections for non-H atoms by using the SHELXL-97 program.[27]

The structure of **19**·0.5 $CH_3COOC_2H_5$ shows a statistical disorder for the $-CH_2$-CH_3 group of the pendant propyl moiety. For these atoms, two different positions were refined with site occupation factors of 0.54(1) and 0.46(1), respectively. The atoms of the ethyl acetate moiety have been treated with a common site occupation factor that has been refined to 0.47(1).

Crystallographic data (excluding structure factors) for both the crystal structures reported in this article have been deposited with the Cambridge Crystallographic Data Centre as supplementary publication numbers CCDC600440 (**19**·0.5 $CH_3COOC_2H_5$) and CCDC600439 (**21**·H_2O). Copies of the data can be obtained, free of charge, on application to CCDC, 12 Union Road, Cambridge CB2 1EZ, U.K. (fax: 144-(0)1223−336033 or e-mail: deposit@ccdc.cam.ac.uk).

Biological Methods. Angiotensin II Receptor Binding Assay.[15] Male Wistar rats (Charles River, Calco, Italy) were killed by decapitation, and their livers were rapidly removed. Angiotensin II receptors from rat liver were prepared by differential centrifugation. The liver was dissected free of fatty tissue and minced accurately with small scissors, and about 3 g of tissue were homogenized by Polytron Ultra-Turrax (maximal speed for 2 × 30 s) in ice cold 20 vol of 5 mM Tris-HCl and 0.25 M sucrose (pH 7.4). The homogenate was centrifuged at 750*g* for 10 min, and the supernatant was filtered through cheesecloth and saved. The pellets were homogenized and centrifuged as before. The combined supernatants were centrifuged at 50 000*g* for 15 min. The resulting pellet was resuspended in 5 mM Tris-HCl and 0.25 M sucrose (pH 7.4) and centrifuged as above. The final pellets were used immediately or stored frozen at −70 °C before use. The membrane pellets were resuspended in the assay buffer (50 mM Tris-HCl, 100 mM NaCl, 10 mM $MgCl_2$, 1 mM EDTA, 100 μM bacitracin, 100 μM PMSF, 0.1% BSA at pH 7.4) to obtain a final protein concentration of 0.25 mg/mL. The binding of [^{125}I]Sar^1,Ile^8-Angiotensin II (Perkin-Elmer Life and Analytical Sciences, S. A. 2000 Ci/mmol) to liver membranes was performed at 25 °C for 180 min in 96-well filtration plates (Millipore GFB-Multiscreen). Each 250 μL incubate contained the following: [^{125}I]Sar^1,Ile^8-Angiotensin II (25 pM), liver membrane proteins (25 μg), and standard or test compounds. Nonspecific binding was measured in the presence of 1 μM Angiotensin II and represented 5−10% of total binding. Binding was terminated by rapid vacuum filtration using a Millipore Multiscreen device. The receptor−ligand complex trapped on filters was washed twice with 200 μL of ice-cold 100 mM NaCl and 100 mM $MgCl_2$. Dried filters disks were punched out and counted in a gamma-counter with 92% efficiency. The IC_{50} value (concentration for 50% displacement of the specifically bound [^{125}I]Sar^1,Ile^8-Angiotensin II) was estimated for the linear portion of the competition curves.

To evaluate the effect of depolymerization of poly-**6c**, stock solutions of **6c** and poly-**6c** in 40% (v/v) DMSO in buffer (50 mM Tris-HCl, 100 mM NaCl, 10 mM $MgCl_2$, 1 mM EDTA, pH 7.4) were freshly prepared, divided into aliquots, and stored at 37 °C for 3 or 6 days. The day of the assay, the solutions were diluted in assay buffer (working solutions) and tested. The final DMSO concentrations did not significantly interfere with the [^{125}I]Sar^1,-Ile^8-Angiotensin II specific binding.

Angiotensin II Functional Antagonism in Rabbit Aorta Strips.[15] New Zealand White rabbits (3−4 kg of body weight, Harlan Italy) were killed by cervical dislocation, after a slight ether anaesthesia. The descending thoracic aorta, with the endothelium removed, was cut into helical strips 3 to 4 mm wide and 15 to 20 mm long. These strips were mounted in 20-mL tissue baths containing Krebs−Henseleit solution of the following composition (mM): NaCl 118; KCl 4.69; KH_2PO_4 1.17; $MgSO_4 \cdot 7\ H_2O$ 1.17; $CaCl_2 \cdot 2\ H_2O$ 2.51; $NaHCO_3$ 25; glucose 11.1. The tissue baths were kept at 37 °C and aerated with 95% O_2 and 5% CO_2. Each strip was connected to an isometric transducer (Basile, Italy), and a resting tension of 2 g was applied to the tissues. Changes in isometric tension were displayed on a 4-channel pen recorder (Basile, Italy). The tissues were allowed to equilibrate for 1 h and were washed every 10 min. The strips were then stimulated by increasing concentrations of angiotensin II to obtain a cumulative concentration−response curve. After 30 min of washout, submaximal-effect (70−80%) concentration of Angiotensin II was chosen to test the inhibitory effects of the substances under study. Various concentrations of the antagonists or vehicles were added, and 60 min contact with the tissues was allowed before adding the agonist to the bathing fluid. Only one antagonist concentration was tested on each tissue preparation. The antagonist activity was expressed as percentage of inhibition of the agonist contractions. The regression line was calculated, and the concentration effective in inhibiting the effect of the agonist by 50% (IC_{50}) was calculated from the regression line.

Intestinal Permeability Experiments In Vitro. The permeability studies were performed with Caco-2 monolayers as described in the literature.[20] Caco-2 cells were cultured in supplemented Dulbecco's modified eagle medium with 10% fetal bovine serum and seeded onto polycarbonate membranes for test compound transport experiments. Caco-2 cell membranes were grown by seeding on Snapwell supports incubated at 37 °C with 5% CO_2/95% O_2 and approximately 95% humidity for 15 to 21 days. Drug permeability experiments were performed at 37 °C at a final drug concentration of 10−100 μM in HBSS buffer (1% DMSO) in the apical chamber (donor side in the apical to basolateral (a−b) permeability study). These concentrations did not show any cytotoxic effect on Caco-2 cells. The samples were obtained from the apical side and from the basolateral chamber at regular time intervals and snap frozen on dry ice/methanol. Drug concentrations

were determined by HPLC-MS. [^{14}C]Mannitol permeability was used as a parameter for assessing monolayer integrity, and propanolol and vinblastine were evaluated as controls. Caco-2 apparent permeability values (P_{app}) were calculated by means of the following equation

$$P_{app} = \frac{\Delta Q}{\Delta t}\frac{1}{AC_0} \quad (1)$$

where $\Delta Q/\Delta t$ was the rate of appearance of the drug in the receiver chamber, C_0 was the initial concentration of the drug in the donor chamber, and A was the surface area of the monolayer. All P_{app} values were standardized and reported as 10^{-6} cm/s.

Pharmacokinetics in Rats. Compounds were either orally administered or injected through the tail vein to fasted Sprague−Dawley rats weighing 250−300 g. After the administration, blood samples were taken at selected times, and the plasma content was analyzed by HPLC, followed by $t_{1/2}$ and area under curve calculations (AUC).

Computational Methods. All molecular modeling studies were performed as previously described[10] using Catalyst 4.7[19] installed on a Silicon Graphic O2 desktop workstation equipped with a 200 MHz MIPS R5000 processor (128 MB RAM) running the Irix 6.5 operating system. All 2D chemical structures were produced within the ISIS/Draw2.1 drawing program.[28]

Acknowledgment. Thanks are due to Italian MIUR (PRIN) for financial support. Professor Stefania D'Agata D'Ottavi's careful reading of the manuscript is also acknowledged.

Supporting Information Available: Full experimental details for the synthesis and the characterization of **5** and **6** and related compounds (chemistry, NMR, MS). This material is available free of charge via the Internet at http://pubs.acs.org.

References

(1) De Gasparo, M.; Catt, K. J.; Inagami, T.; Wright, J. W.; Unger, T. International Union of Pharmacology. XXIII. The Angiotensin II Receptors. *Pharmacol. Rev*. **2000**, *52*, 415−472 and references therein.

(2) Inoue, Y.; Nakamura, N.; Inagami, T. A Review of Mutagenesis Studies of Angiotensin II Type 1 Receptor, the Three-Dimensional Receptor Model in Search of the Agonist Binding Site and the Hypothesis of a Receptor Activation Mechanism. *J. Hypertens*. **1997**, *15*, 703−714.

(3) (a) Wexler, R. R.; Greenlee, W. J.; Irvin, J. D.; Goldberg, M. R.; Prendergast, K.; Smith, R. D.; Timmermans, P. B. M. W. M. Nonpeptide Angiotensin II Receptor Antagonists: The Next Generation in Antihypertensive Therapy. *J. Med. Chem*. **1996**, *39*, 625−656. (b) Schmidt, B.; Schieffer, B. Angiotensin II AT1 Receptor Antagonist. Clinical Implications of Active Metabolites. *J. Med. Chem*. **2003**, *46*, 2261−2270, and references therein.

(4) (a) Mantlo, N. B.; Chakravarty, P. K.; Ondeyka, D. L.; Siegl, P. K. S.; Chang, R. S.; Lotti, V. J.; Faust, K. A.; Chen, T.-B.; Schorn, T. W.; Sweet, C. S.; Emmert, S. E.; Patchett, A. A.; Greenlee, W. J. Potent, Orally Active Imidazo[4,5-*b*]pyridine-Based Angiotensin II Receptor Antagonists. *J. Med. Chem*. **1991**, *34*, 2919−2922. (b) Kim, D.; Mantlo, N. B.; Chang, R. S.; Kivlighn, S. D.; Greenlee, W. J. Evaluation of Heterocyclic Acid Equivalents as Tetrazole Replacements in Imidazopyridine-Based Nonpeptide Angiotensin II Receptor Antagonists. *Bioorg. Med. Chem. Lett*. **1994**, *4*, 41−44.

(5) Mantlo, N. B.; Chang, R. S. L.; Siegl, P. K. S. Angiotensin II Receptor Antagonists Containing a Phenylpyridine Element. *Bioorg. Med. Chem. Lett*. **1993**, *3*, 1693−1696.

(6) Cappelli, A.; Pericot Mohr, G.; Gallelli, A.; Rizzo, M.; Anzini, M.; Vomero, S.; Mennuni, L.; Ferrari, F.; Makovec, F.; Menziani, M. C.; De Benedetti, P. G.; Giorgi, G. Design, Synthesis, Structural Studies, Biological Evaluation, and Computational Simulations of Novel Potent AT_1 Angiotensin II Receptor Antagonists Based on the 4-Phenylquinoline Structure. *J. Med. Chem*. **2004**, *47*, 2574−2586.

(7) Rizzo, M.; Anzini, M.; Cappelli, A.; Vomero, S.; Ventrice, D.; De Sarro, G.; Procopio, S.; Costa, N.; Makovec, F. Determination of a Novel Angiotensin-AT_1 Antagonist CR3210 in Biological Samples by HPLC. *Il Farmaco*. **2003**, *58*, 837−844.

(8) Rizzo, M.; Ventrice, D.; Monforte, F.; Procopio, S.; De Sarro, G.; Anzini, M.; Cappelli, A.; Makovec, F. Sensitive SPE-HPLC Method to Determine a Novel Angiotensin-AT_1 Antagonist in Biological Samples. *J. Pharm. Biomed. Anal*. **2004**, *35*, 321−329.

(9) As far as the pharmacokinetic properties are concerned, it should be noted that even the marketed AT_1 receptor antagonists show limited oral bioavailability (eprosartan 13%, valsartan 25%, losartan 33%, candesartan 42%, telmisartan 50%, and irbesartan 60−80%). ((a) Israili, Z. H. Clinical Pharmacokinetics of Angiotensin II (AT1) Receptor Blockers in Hypertension. *J. Hum. Hypertens*. **2000**, *14*, S73−S86. (b) Brunner, H. R. The New Angiotensin II Receptor Antagonist, Irbesartan. *Am. J. Hypertens*. **1997**, *10*, 311S−317S.) Furthermore, losartan exhibiting highly variable oral bioavailability is transported by *P*-glycoprotein, whereas its carboxylic acid metabolite is not a *P*-glycoprotein substrate (Soldner, A.; Benet, L. Z.; Mutschler, E.; Christians, U. Active Transport of the Angiotensin-II Antagonist Losartan and Its Main Metabolite EXP 3174 Across MDCK-MDR1 and Caco-2 Cell Monolayers. *Br. J. Pharmacol*. **2000**, *129*, 1235−1243).

(10) Krovat, E. M.; Langer, T. Non-Peptide Angiotensin II Receptor Antagonists: Chemical Feature Based Pharmacophore Identification. *J. Med. Chem*. **2003**, *46*, 716−726.

(11) Natsugari, H.; Ikeura, Y.; Kiyota, Y.; Ishichi, Y.; Ishimaru, T.; Saga, O.; Shirafuji, H.; Tanaka, T.; Kamo, I.; Doi, T.; Otsuka, M. Novel, Potent, and Orally Active Substance P Antagonists: Synthesis and Antagonist Activity of *N*-Benzylcarboxamide Derivatives of Pyrido-[3,4-*b*]pyridine. *J. Med. Chem*. **1995**, *38*, 3106−3120.

(12) (a) Senanayake, C. H.; Fredenburgh, L. E.; Reamer, R. A.; Liu, J.; Roberts, F. E.; Humphrey, G.; Thompson, A. S.; Larsen, R. D.; Verhoeven, T. R.; Reider, P. J.; Shinkai, I. New Approach to the Imidazolutidine Moiety of MK-996. *Heterocycles* **1996**, *42*, 821−830. (b) Chakravarty, P. K.; Greenlee, W. J.; Mantlo, N. B.; Patchett, A. A.; Walsh, T. F. Substituted Imidazo-Fused 6-Membered Heterocycles as Angiotensin II Antagonists. U.S. Patent 5,332,744, 1994.

(13) Cappelli, A.; Pericot Mohr, G.; Anzini, M.; Vomero, S.; Donati, A.; Casolaro, M.; Mendichi, R.; Giorgi, G.; Makovec, F. Synthesis and Characterization of a New Benzofulvene Polymer Showing a Thermoreversible Polymerization Behavior. *J. Org. Chem*. **2003**, *68*, 9473−9476.

(14) Cappelli, A.; Anzini, M.; Vomero, S.; Donati, A.; Zetta, L.; Mendichi, R.; Casolaro, M.; Lupetti, P.; Salvatici, P.; Giorgi, G. New π-Stacked Benzofulvene Polymer Showing Thermoreversible Polymerization: Studies in Macromolecular and Aggregate Structures and Polymerization Mechanism. *J. Polym. Sci., Part A: Polym. Chem*. **2005**, *43*, 3289−3304.

(15) (a) Chang, R. S. L.; Siegl, P. K. S.; Clineschmidt, B. W.; Mantlo, N. B.; Chakravarty, P. K.; Greenlee, W. J.; Patchett, A. A.; Lotti, V. J. In vitro Pharmacology of L-158,809, a New Highly Potent and Selective Angiotensin II Receptor Antagonists. *J. Pharmacol. Exp. Ther*. **1992**, *262*, 133−138. (b) Robertoson, M. J.; Cunoosamy, M. P.; Clark, K. L. Effects of Peptidase Inhibition on Angiotensin Receptor Agonist and Antagonist Potency in Rabbit Isolated Thoracic Aorta. *Br. J. Pharmacol*. **1992**, *106*, 166−172.

(16) Naphthalene derivative **4a** was described in a patent application and resynthesized in our laboratory as a reference compound for our quinoline derivatives (Suzuki, K.; Fujiwara, S.; Machii, D.; Ochifuji, N.; Takai, H.; Oono, T.; Furuta, S.; Yamada, K. Preparation of Imidazopyridines and Analogs as Angiotensin II Antagonists. Jpn. Kokai Tokkyo Koho JP 06 92,939, 1994. and Fujiwara, S.; Takai, H.; Mizukami, T.; Myaji, H.; Sato, S.; Oomori, T.; Nukui, E. Preparation of N-[4-(4-Quinolinyl)benzyl]benzimidazole Derivatives as Immunosuppressants. Jpn. Kokai Tokkyo Koho JP 06, 340,658, 1994.)

(17) Almansa, C.; Gómez, L. A.; Cavalcanti, F. L.; de Arriba, A. F.; Rodríguez, R.; Carceller, E.; García-Rafanell, J.; Forn, J. Diphenylpropionic Acids as New AT_1 Selective Angiotensin II Antagonists. *J. Med. Chem*. **1996**, *39*, 2197−2206.

(18) Carini, D. J.; Duncia, J. V.; Aldrich, P. E.; Chiu, A. T.; Johnson, A. L.; Pierce, M. E.; Price, W. A.; Santella, J. B., III; Wells, G. J.; Wexler, R. R.; Wong, P. C.; Yoo, S.-E.; Timmermans, P. B. M. W. M. Nonpeptide Angiotensin II Receptor Antagonists: The Discovery of a Series of N-(Biphenylmethyl)imidazoles as Potent, Orally Active Antihypertensives. *J. Med. Chem*. **1991**, *34*, 2525−2547.

(19) *Catalyst*, version 4.7 (software package); Accelrys, Inc. (previously known as Molecular Simulations, Inc.): San Diego, CA 2002.

(20) (a) Artursson, P. Epithelial Transport of Drugs in Cell Culture. I: A Model for Studying the Passive Diffusion of Drugs over Intestinal Absorptive (Caco-2) Cells. *J. Pharm. Sci*. **1990**, *79*, 476−482. (b) Artursson, P.; Karlsson, J. Correlation between Oral Drug Absorption in Humans and Apparent Drug Permeability Coefficients in Human Intestinal Epithelial (Caco-2) Cells. *Biochem. Biophys. Res. Commun*. **1991**, *175*, 880−885.

(21) Ribadeneira, M. D.; Aungst, B. J.; Eyermann, C. J.; Huang, S.-M. Effects of Structural Modifications on the Intestinal Permeability of Angiotensin II Receptor Antagonists and the Correlation of In Vitro, In Situ, and In Vivo Absorption. *Pharm. Res*. **1996**, *13*, 227−233.
(22) Comparative studies on the UDP-glucuronosyltransferase-dependent metabolism revealed that intrinsic clearance ($CL_{intrinsic} = V_{max}/K_m$) of compound **4b** is 7-fold higher than that shown by **2a** (Valoti, M. Personal communication). Interestingly, other authors reported that the absence of **2a** glucuronide in the hepatocyte and its presence in the bile suggest that its rate of formation is much slower than its rate of transport out of the cell (see ref 23).
(23) (a) Colletti, A. E.; Krieter, P. A. Disposition of Angiotensin II Receptor Antagonist L-158,809 in Rats and Rhesus Monkeys. *Drug Metab. Disp*. **1994**, *22*, 183−188. (b) Huskey, S. W.; Miller, R. R.; Chiu, S.-H. L. N-Glucuronidation Reactions. I. Tetrazole N-Glucuronidation of Selected Angiotensin II Receptor Antagonists in Hepatic Microsome from Rats, Dogs, Monkeys, and Humans. *Drug Metab. Dispos*. **1993**, *21*, 792−799 and references therein.
(24) (a) Greer, S. C. Physical Chemistry of Equilibrium Polymerization. *J. Phys. Chem. B* **1998**, *102*, 5413−5422. (b) Ishizone, T.; Ohnuma, K.; Okazawa, Y.; Hirao, A.; Nakahama, S. Anionic Polymerization of Monomers Containing Functional Groups. 12. Anionic Equilibrium Polymerization of 4-Cyano-α-methylstyrene. *Macromolecules* **1998**, *31*, 2797−2803. (c) Iwatsuki, S.; Itoh, T.; Higuchi, T.; Enomoto, K. Equilibrium Polymerization of 7,8-Dibenzoyl-, 7,8-Diacetyl-, and 7,8-Dibutoxycarbonyl-7,8-dicyanoquinodimethane and Their Copolymerization with Styrene: a New Concept on the Mechanism of Alternating Copolymerization. *Macromolecules*, **1988**, *21*, 1571−1579. (d) Dainton, F. S.; Ivin, K. J. Reversibility of the Propagation Reaction in Polymerization Processes and Its Manifestation in the Phenomenon of a 'Ceiling Temperature'. *Nature* **1948**, *162*, 705−707.
(25) For a related pharmacophore model, see Ismail, M. A. H.; Barker, S.; Abou El Ella, D. A.; Abouzid, K. A. M.; Toubar, R. A.; Todd, M. H. Design and Synthesis of New Tetrazolyl- and Carboxy-biphenylmethyl-quinazolin-4-one Derivatives as Angiotensin II AT_1 Receptor Antagonists. *J. Med. Chem*. **2006**, *49*, 1526−1535.
(26) Sheldrick, G. M. *SHELXS-97, Rel. 97-2, A Program for Automatic Solution of Crystal Structures*; University of Göttingen: Göttingen, Germany, 1997.
(27) Sheldrick, G. M. *SHELXL-97, Rel. 97-2, A Program for Crystal Structure Refinement*; University of Göttingen: Göttingen, Germany, 1997.
(28) *ISIS/Draw*, version 2.1; MDL Information Systems: San Diego, CA 1990−1996.

JM0603163